# The FOOT Pixel tracker status

1. Introduction
2. Some results with M28 sensors
   - Measurements with M28s at the LNF BTF in 2015
   - Measurements for PADME with M28s at the LNF BTF in 2017
2. Target and Vertex tracker
   - The FIRST target and Vertex setup
   - The new FOOT arrangement
3. The magnetic region
4. Inner Pixel tracker
5. CDR for the FOOT Pixel tracker
6. LNF 2018 financial request and planning
7. Conclusion

# Introduction

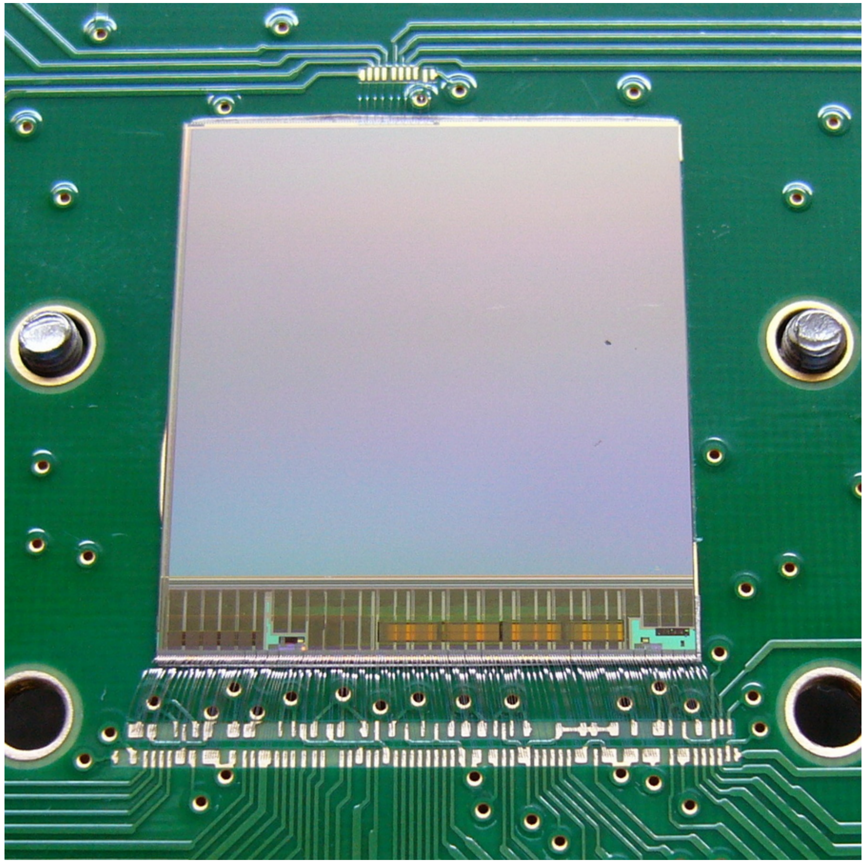

**M28 pixel sensor main characteristics**

- MAPS ( AMS 0.35 µm, 15 µm epi-layer )
- 50 µm thickness
- 928 (rows) x 960 (columns) pixels
- 20.7 µm pitch
- Size 20.22 mm x 22.71 mm
- chip readout time 185.6 µs
- Digital Zero Suppressed Output

**By IPHC In2p3 Strasbourg**

# Measurements with M28s at the LNF BTF in 2015

**Main goal: measurement of spatial resolution and fake hit rate for the double row readout validation**

Critical point => Multiple scattering at 500 MeV electron beam!

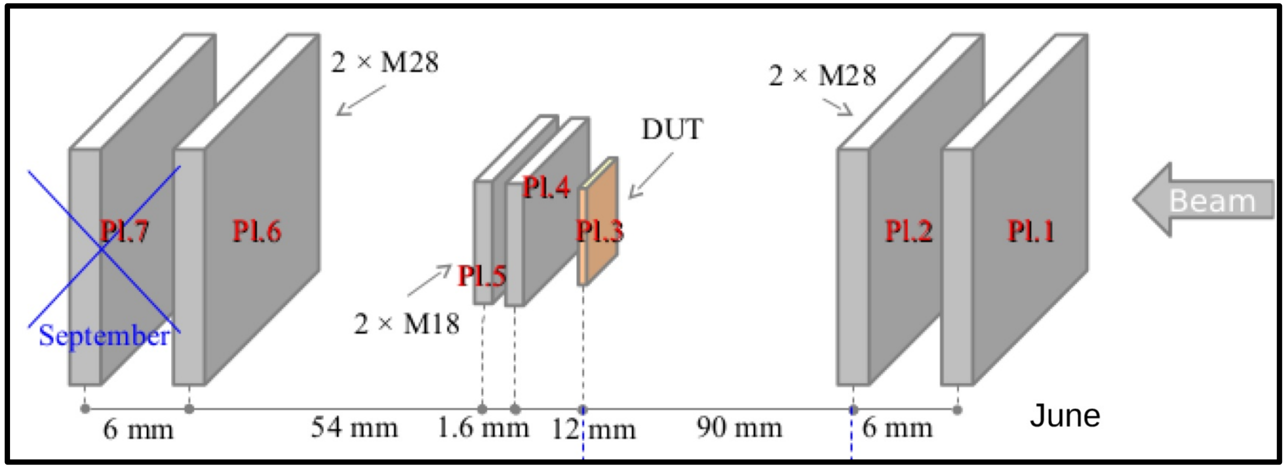


❑ 3 MIMOSA28 planes:
- AMS 0.35 µm OPTO process
- 50 µm thickness
- **960x928 binary pixels**
- **20.7 x 20.7 µm2 pixel pitch**
- **Digital output**
- Readout clock: 80 MHz

❑ 2 MIMOSA18 planes:
- AMS 0.35 µm OPTO process
- 50 µm thickness
- **512x512 binary pixels**
- **10 x 10 µm2 pixel pitch**
- **Analog output**
- Readout clock: 20 MHz

❑ DUT: MIMOSA22ThrB
- Tower-Jazz 0.18 µm process
- 50 µm thickness
- **64×64 elongated pixels: 22 µm (row) × 33 µm (col)**
- **binary readout**
- Readout clock: 100 MHz

# Measurements with M28s at the LNF BTF in 2015

Residual and efficiency as a function of the threshold

Analysis parameters:
Hit-track distance=150 μm
Chi2 cut =4

Efficiency evaluated as:
ϵ = Num. of tracks associated to a hit in the DUT/
Nun. of tracks crossing the DUT
Efficiency error is the binomial distribution variance

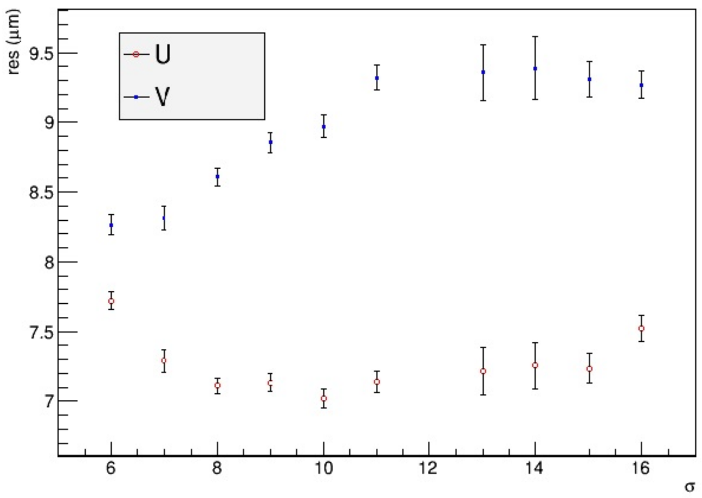


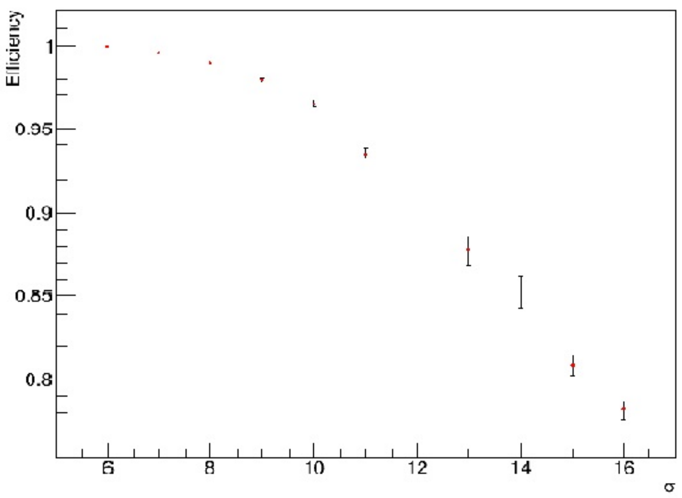


How we disantangle the multiple scattering effect to evaluate the **RESOLUTION** from the obtained **RESIDUALS**?

# Measurements with M28s at the LNF BTF in 2015

**Main goal Evaluate the smearing in the position resolution produced by multiple scatterings of beam e- in the telescope planes (@ BTF).**

**(Exp. Residual)$^2$ = (Intr. Resolution)$^2$ + (Mult. Scatt. Residual)$^2$**

**Procedure**

1. Reproduce the telescope geometry in GEANT (no pixelization introduced)
2. Simulate the beam (electrons)
3. Follow the propagation and the interactions of the beam particles with the materials
4. Save GEANT hit position in each plane
5. Reconstruct the tracks by processing the data with TAF
6. The result is then subtracted to the overall experimental resolution

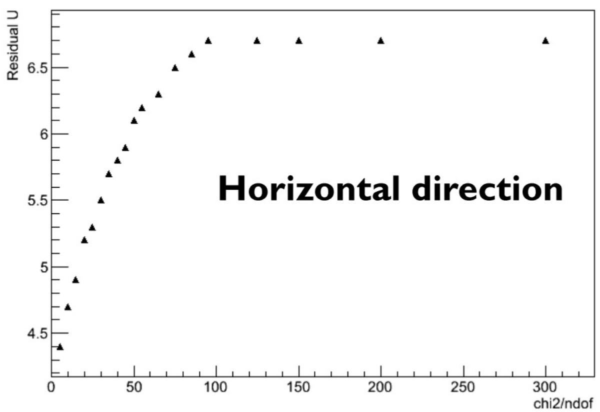


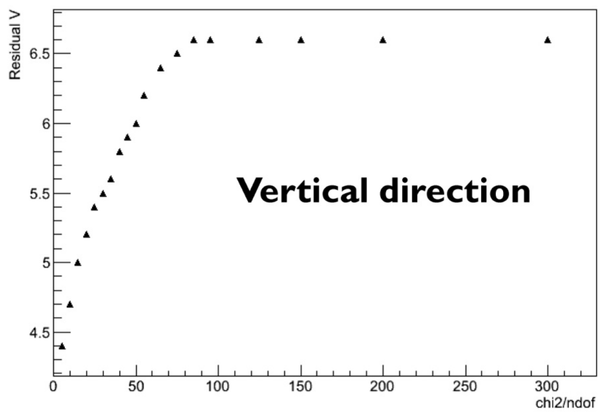

# Measurements with M28s at the LNF BTF in 2015

| | Horizontal coordinate | | | Vertical coordinate | | |
|---|---|---|---|---|---|---|
| **Chi2 cut** | **Exp Resid** | **Sim. Resid.** | **Resolution** | **Exp Resid** | **Sim. Resid.** | **Resolution** |
| 20 | 6.7 | 5.2 | 4.2 | 8.1 | 5.2 | 6.2 |
| 55 | 7.3 | 6.2 | 3.9 | 8.9 | 6.2 | 6.4 |
| 200 | 8.2 | 6.7 | 4.7 | 9.6 | 6.6 | 7.0 |

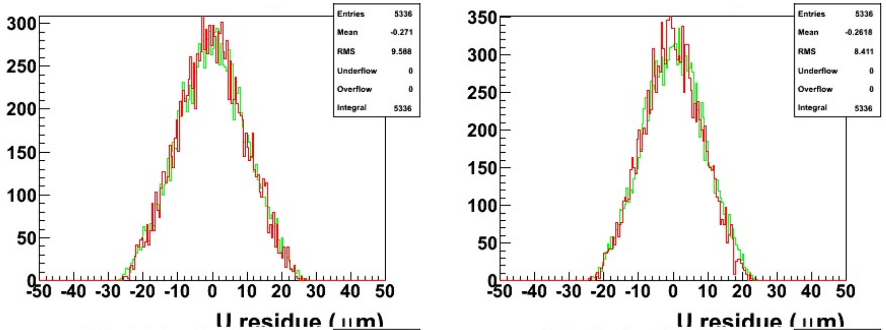


Residual comparison ( data versus GEANT simulation) in the 5 tracking planes in u coordinate

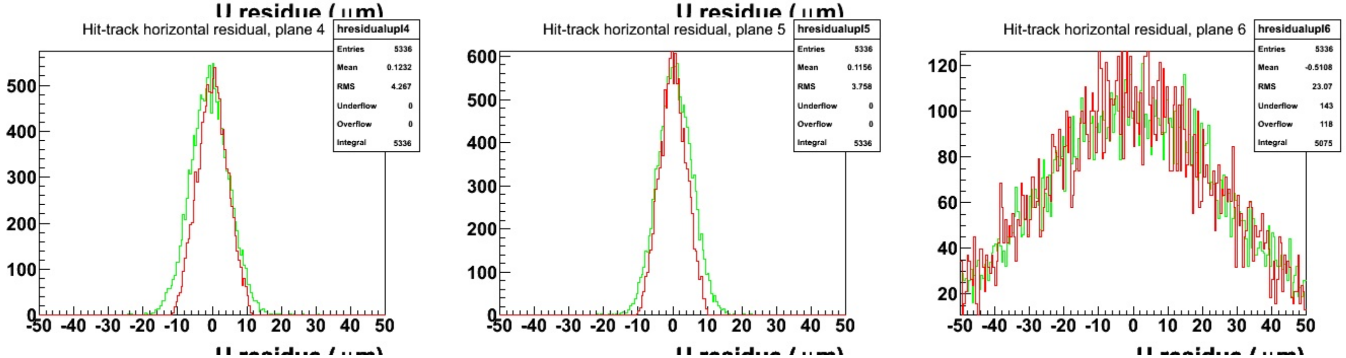

# Measurements for PADME with M28s at the LNF BTF in 2017

# PADME BTF beam monitor
# ( readout system )

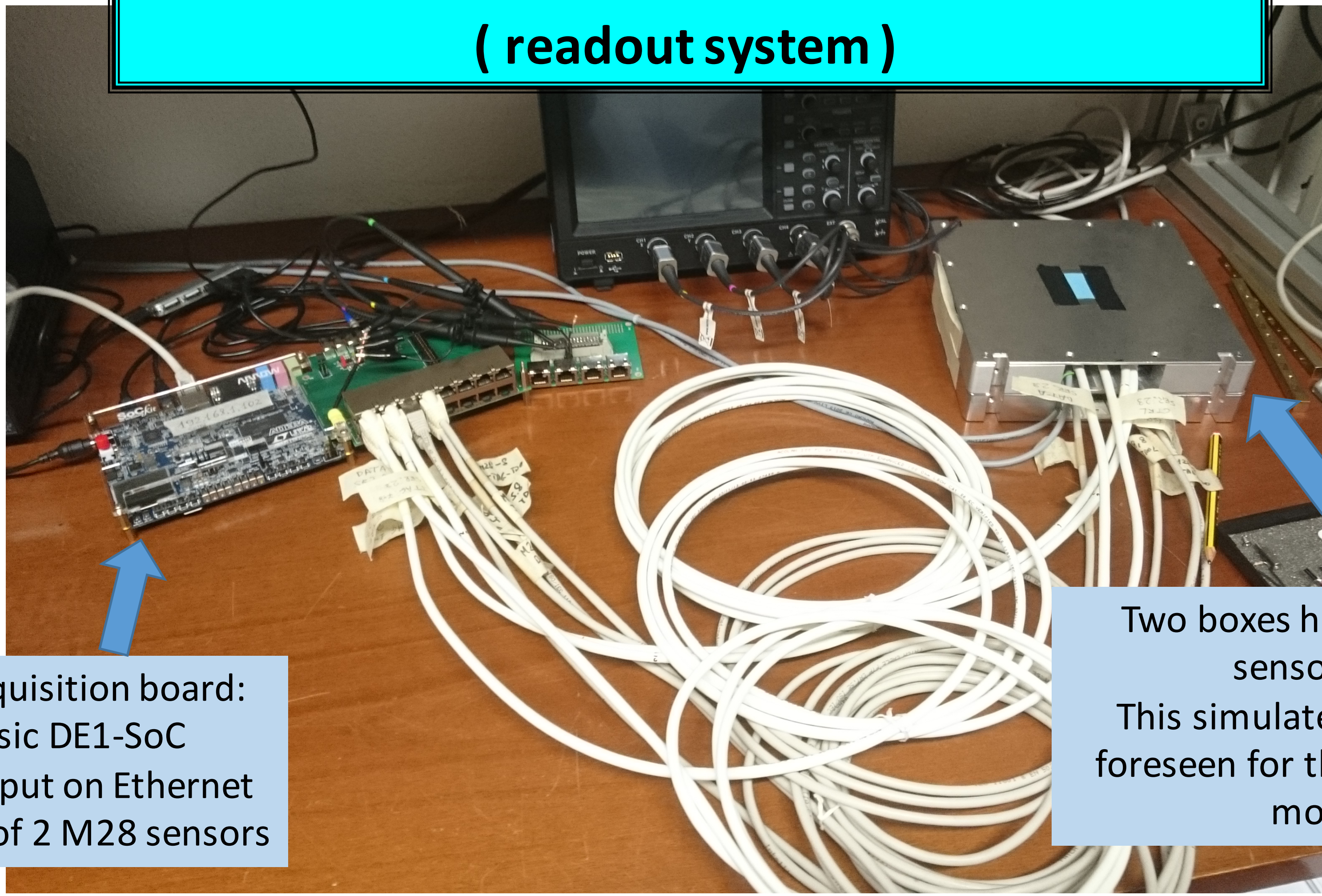

Data acquisition board:
Terasic DE1-SoC
Data output on Ethernet
Readout of 2 M28 sensors

Two boxes housing 2 M28s sensors each.
This simulate the 2 stations foreseen for the PADME beam monitor.

# PADME BTF setup February 2017

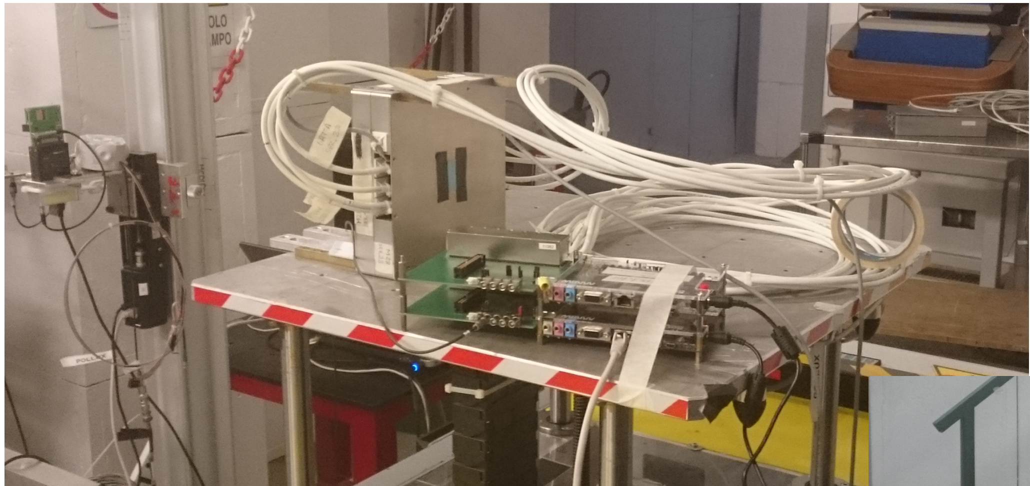

# PADME BTF setup February 2017
# Run 1023 ( 100 Keventi )
# Beam profile in the two M28 sensors

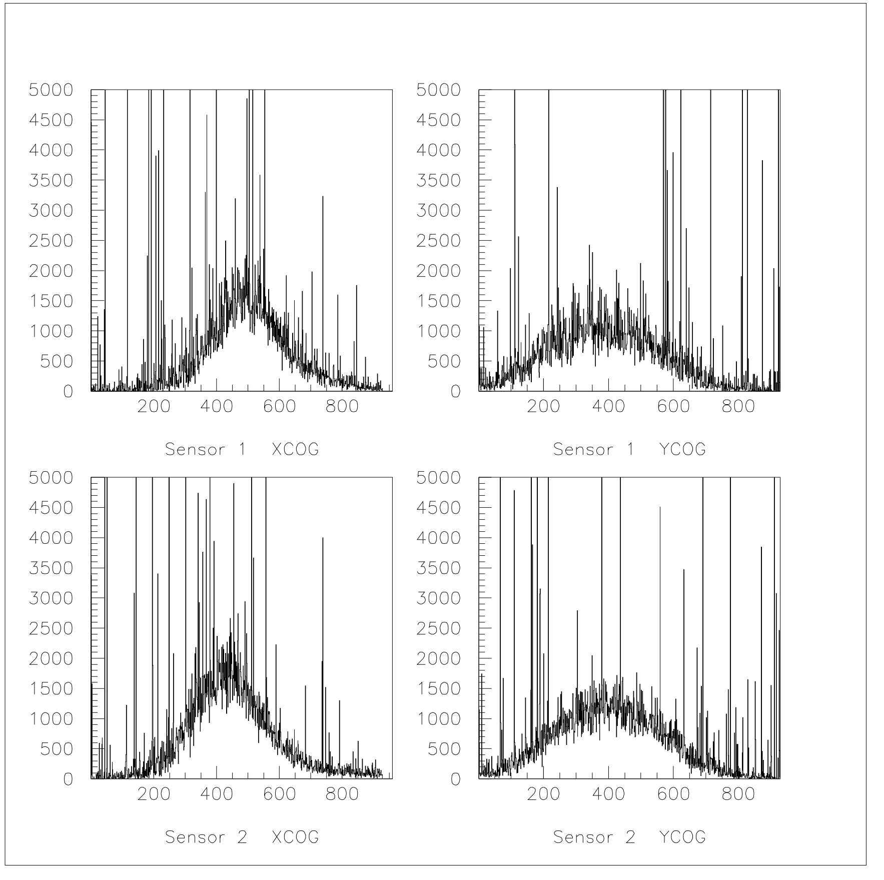

# PADME BTF setup February 2017

**Clusters coordinate correlations between the 2 sensors:**
- **cluster size >=1**
- **cluster size >=2**

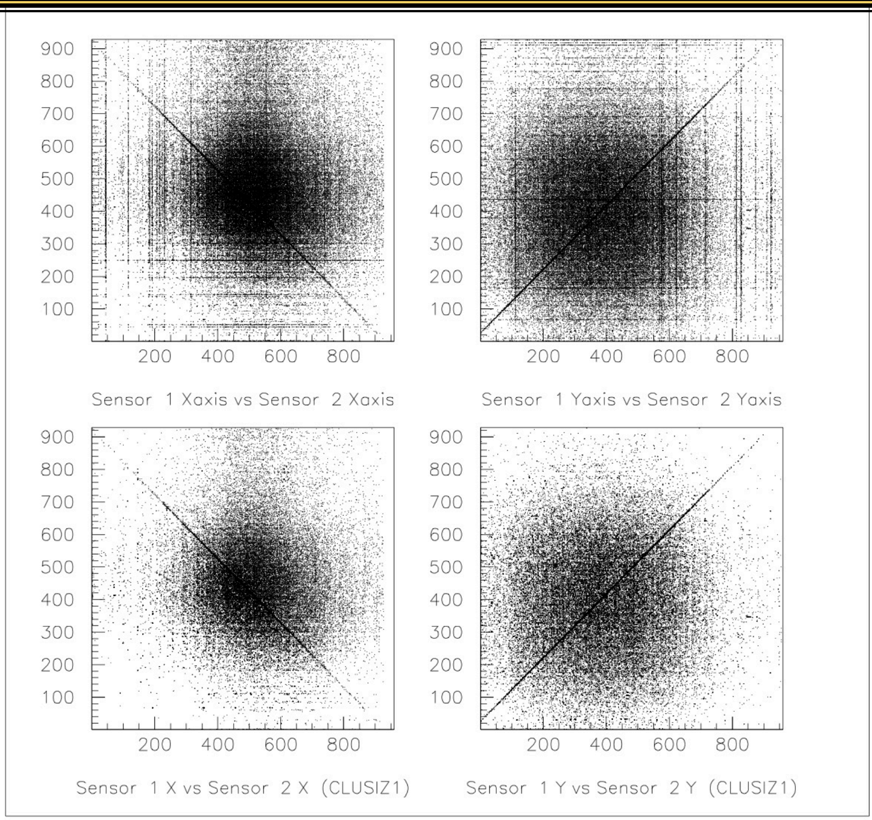


**Clusters coordinate correlations between the 2 sensors :**
- **cluster size >=2**
- **cluster size >=3**

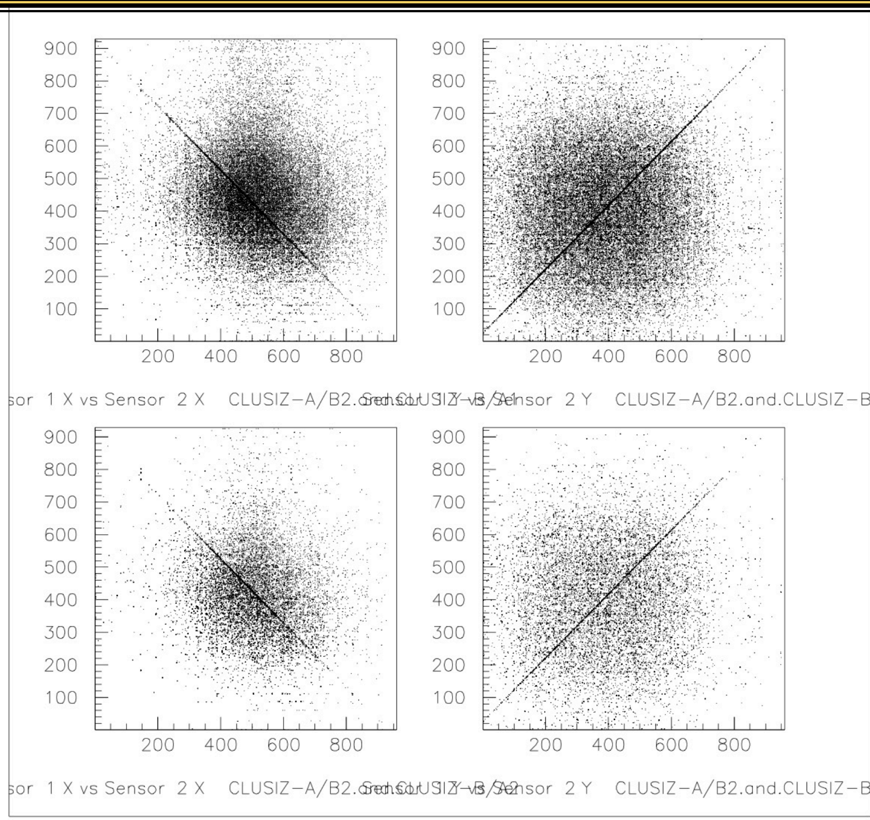

# PADME BTF setup February 2017

**Clusters coordinate correlations between the 2 sensors :**
- **cluster size >=1**
- **cluster size >=2**

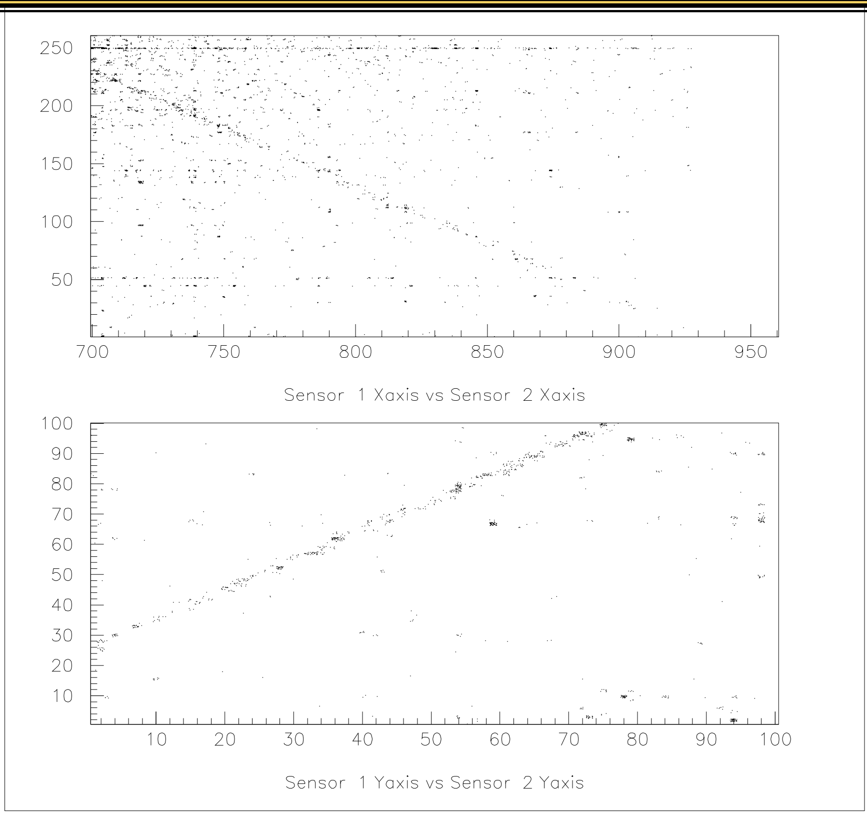


**Summary**

- New DAQ working at 25 Hertz rate ( Tested in lab up to 1 KHz )
- Reliable results froma date first analysis on data quality
- Tracking analysis under way
- Next step: read out of 4 sensors
- Trigger supervisor functionality to be implemented

## PADME BTF February 2017 - Run 1023 ( 100 Keventi ) residuals in the two M28 sensors pre alignment

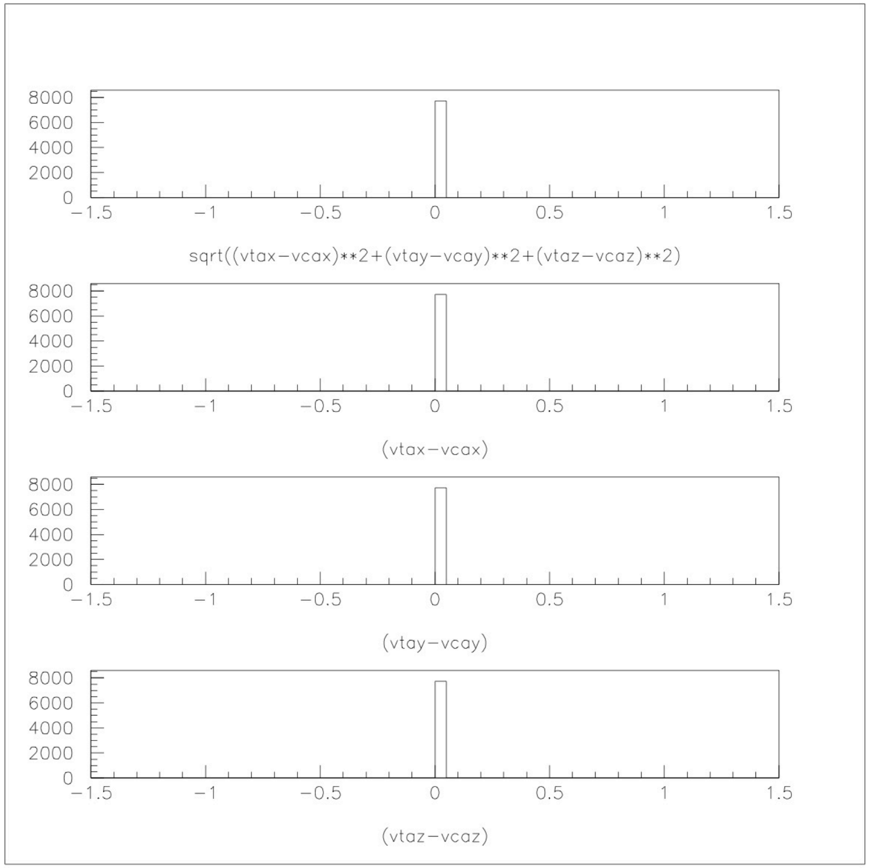


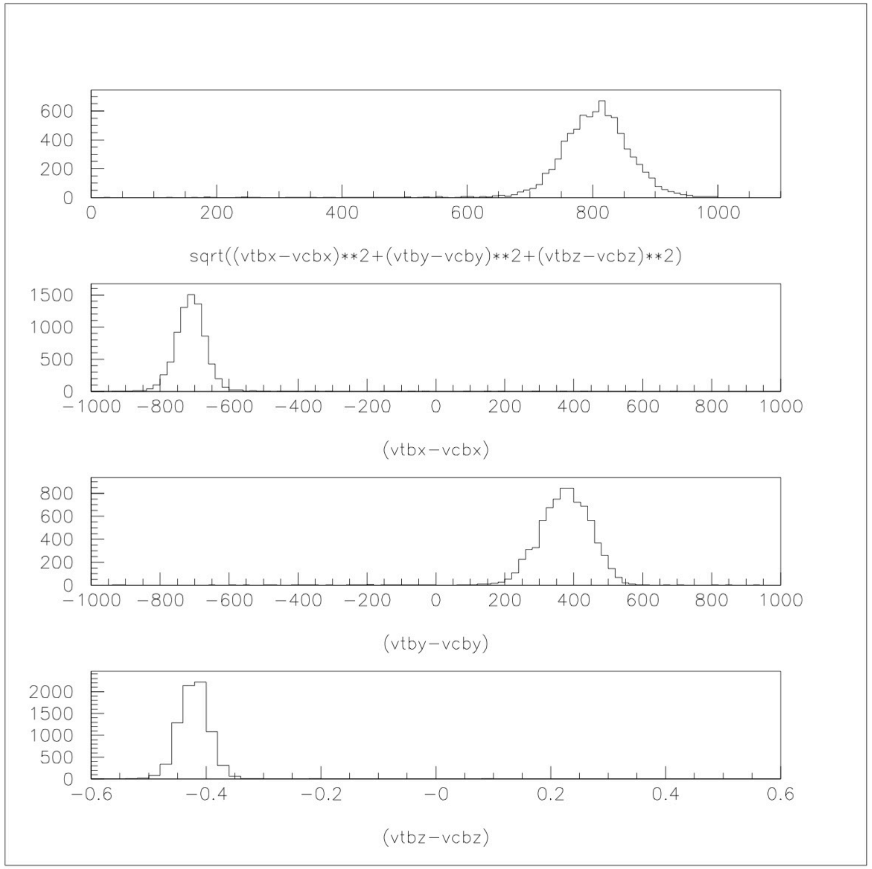

**PADME BTF February 2017 - Run 1023 ( 100 Keventi )**
**residuals in the two M28 sensors pre alignment ( X vs Y plots )**

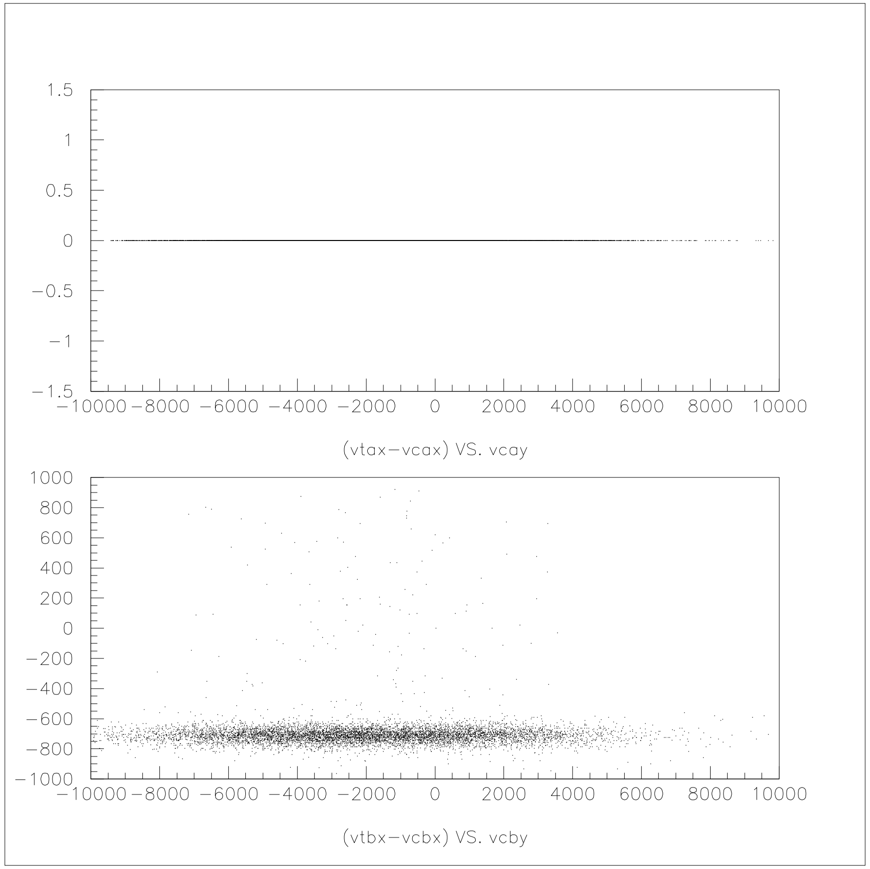


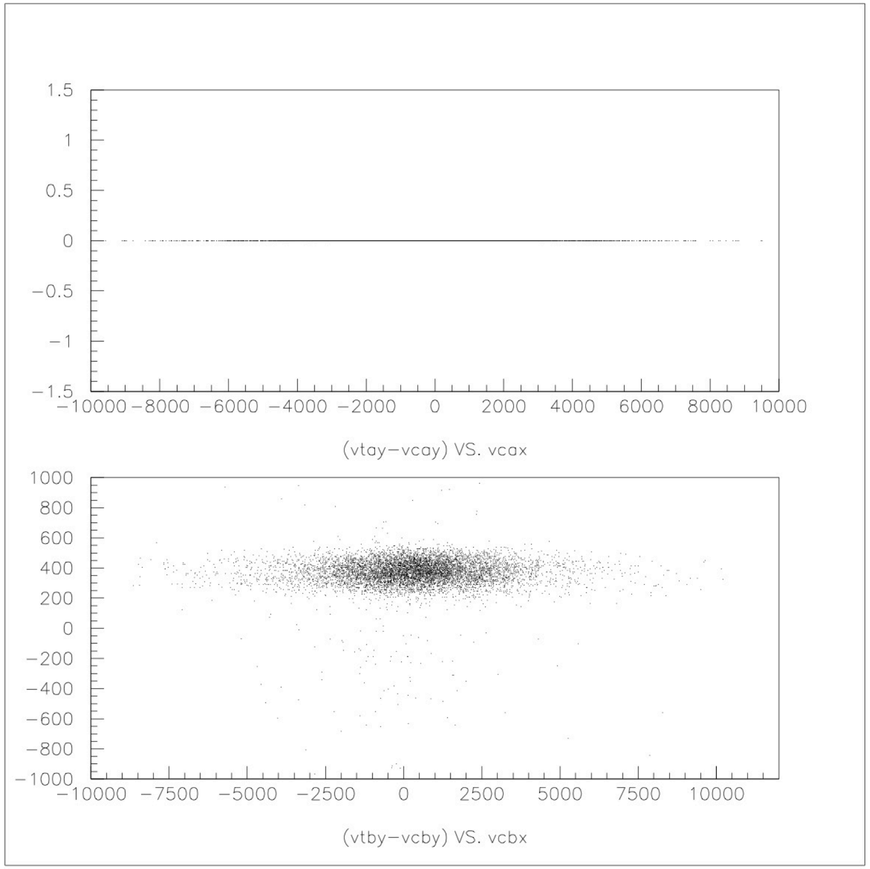

# PADME BTF February 2017 - Run 1023 ( 100 Keventi )
# Beam profile in the two M28 sensors after alignment

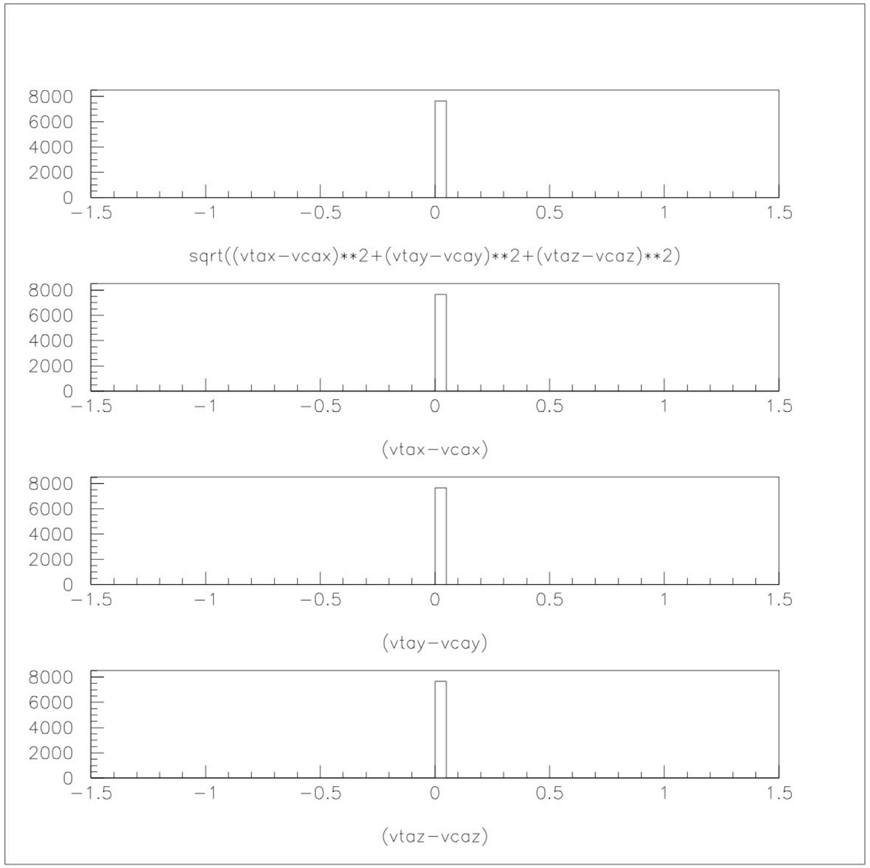


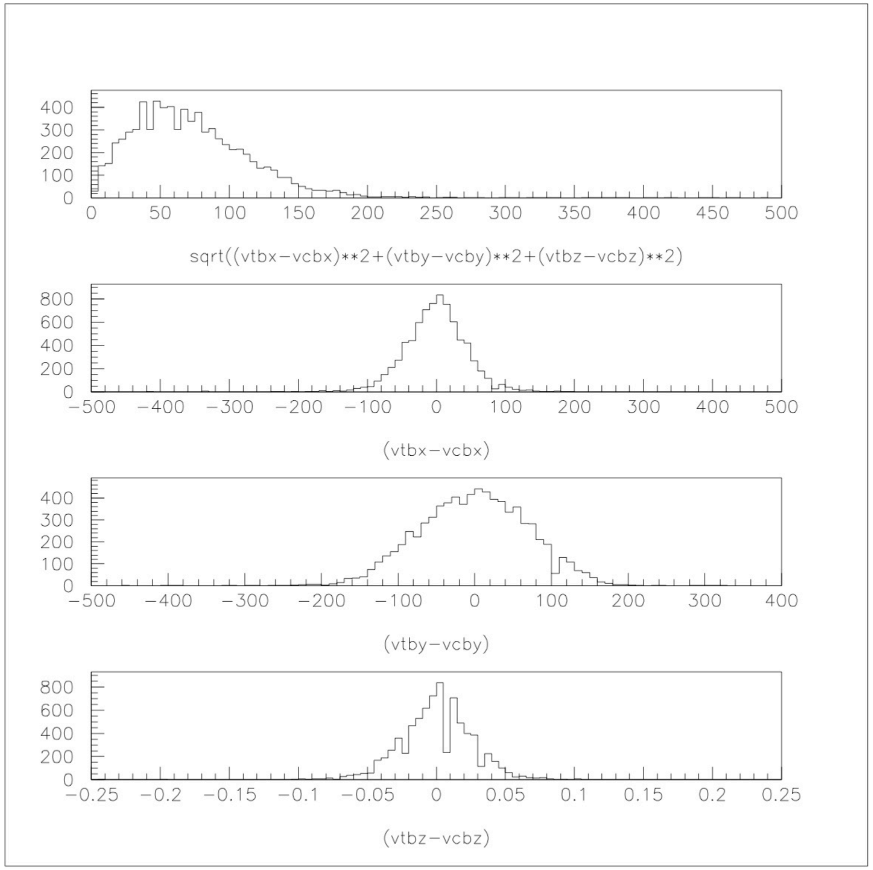

## PADME BTF February 2017 - Run 1023 ( 100 Keventi ) residuals in the two M28 sensors after alignment ( X vs Y plots )

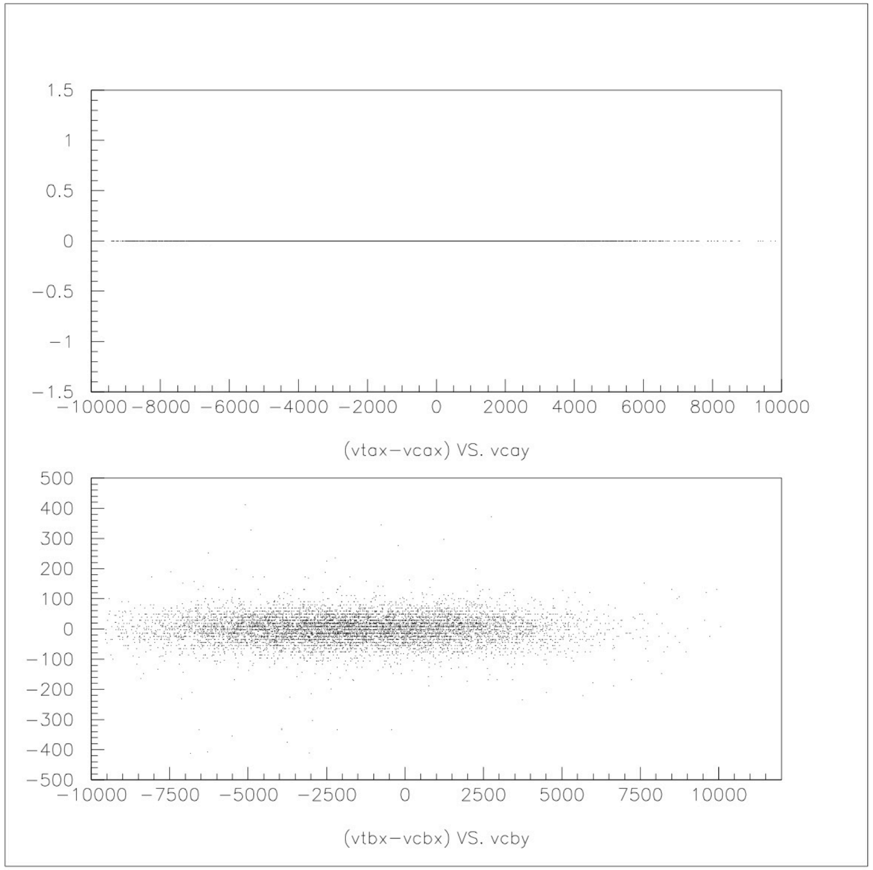


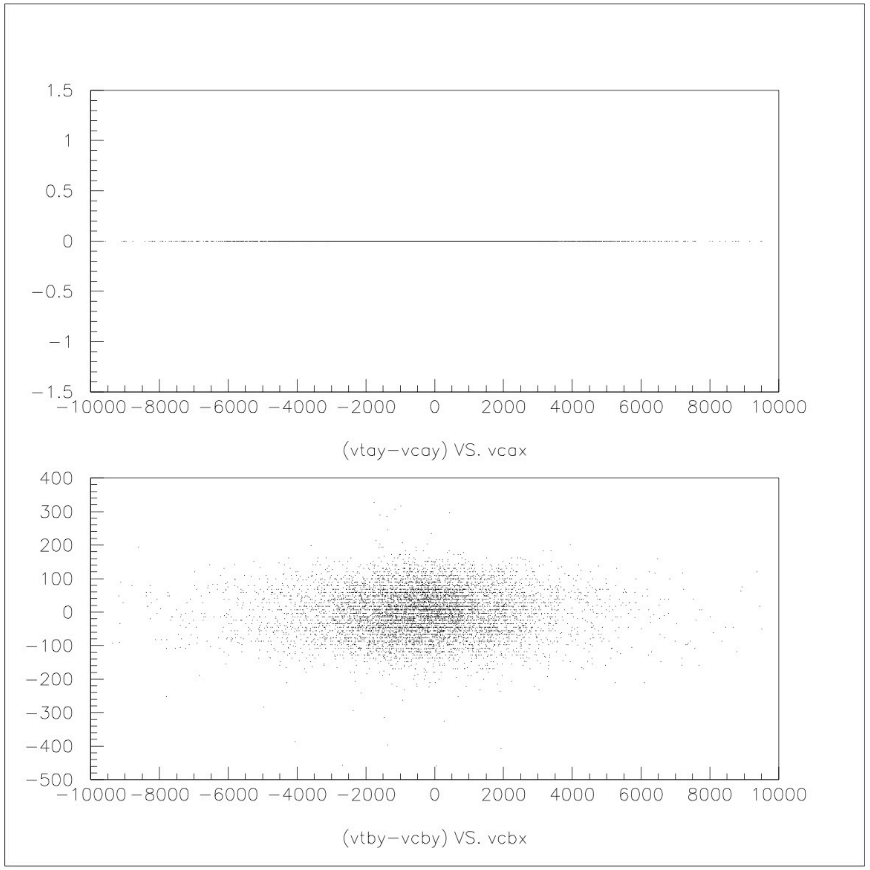

# PADME BTF February 2017 - Run 1023 ( 100 Keventi )
# Beam angular distribution before and after alignment

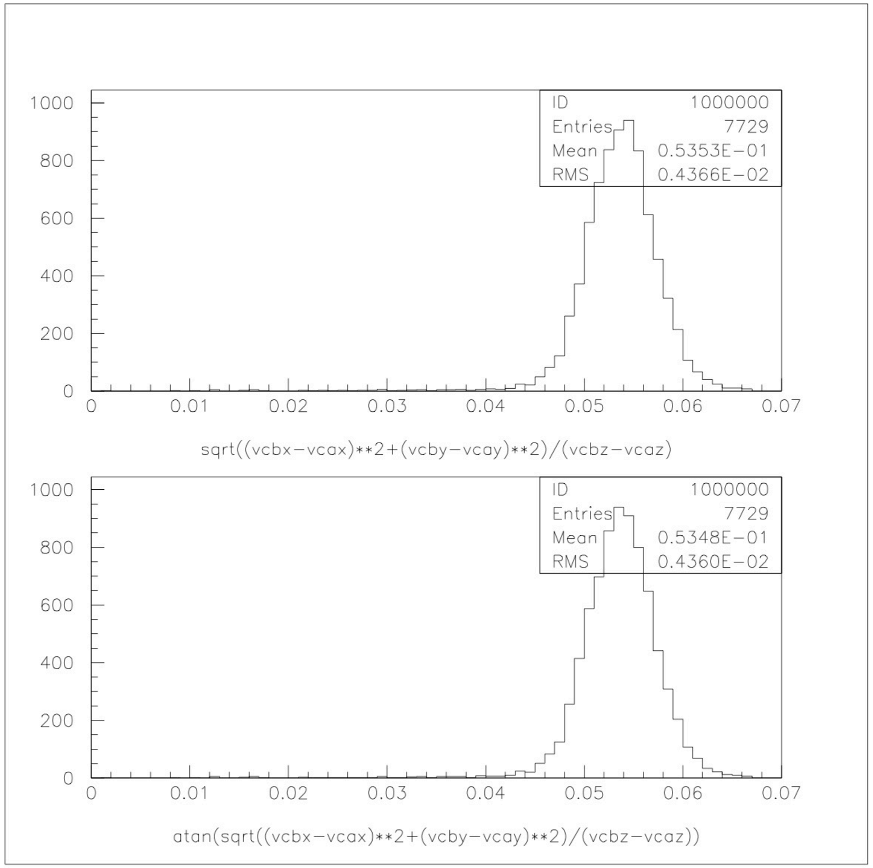


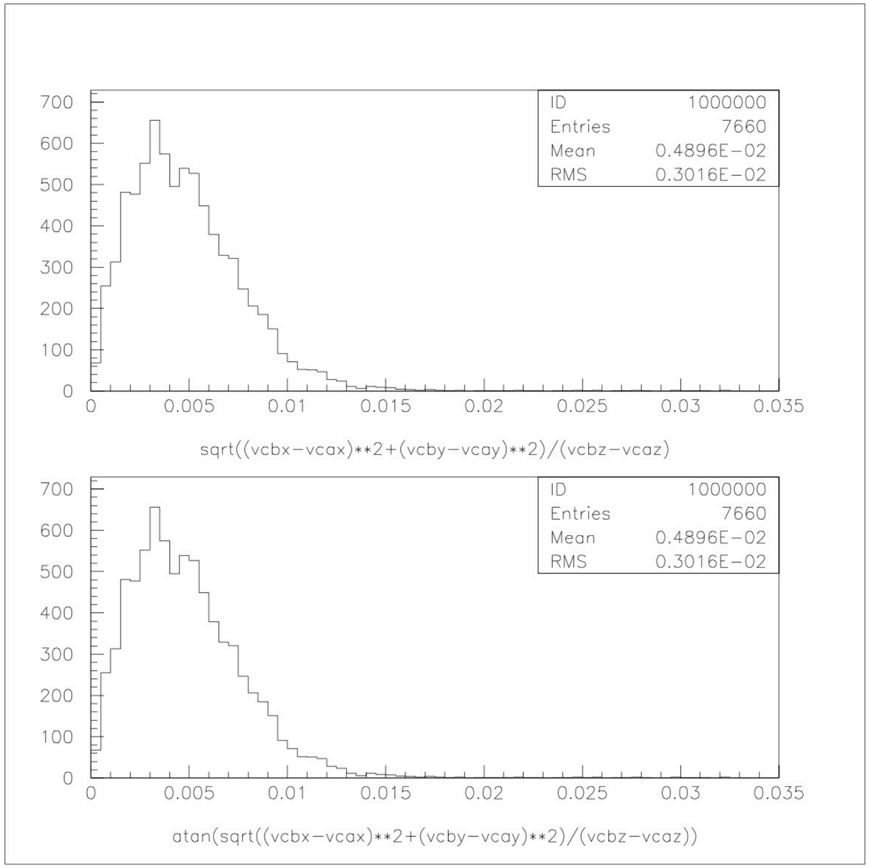

## PADME BTF February 2017 - Run 1023 ( 100 Keventi )
## Geometrical tracks plot 4k events

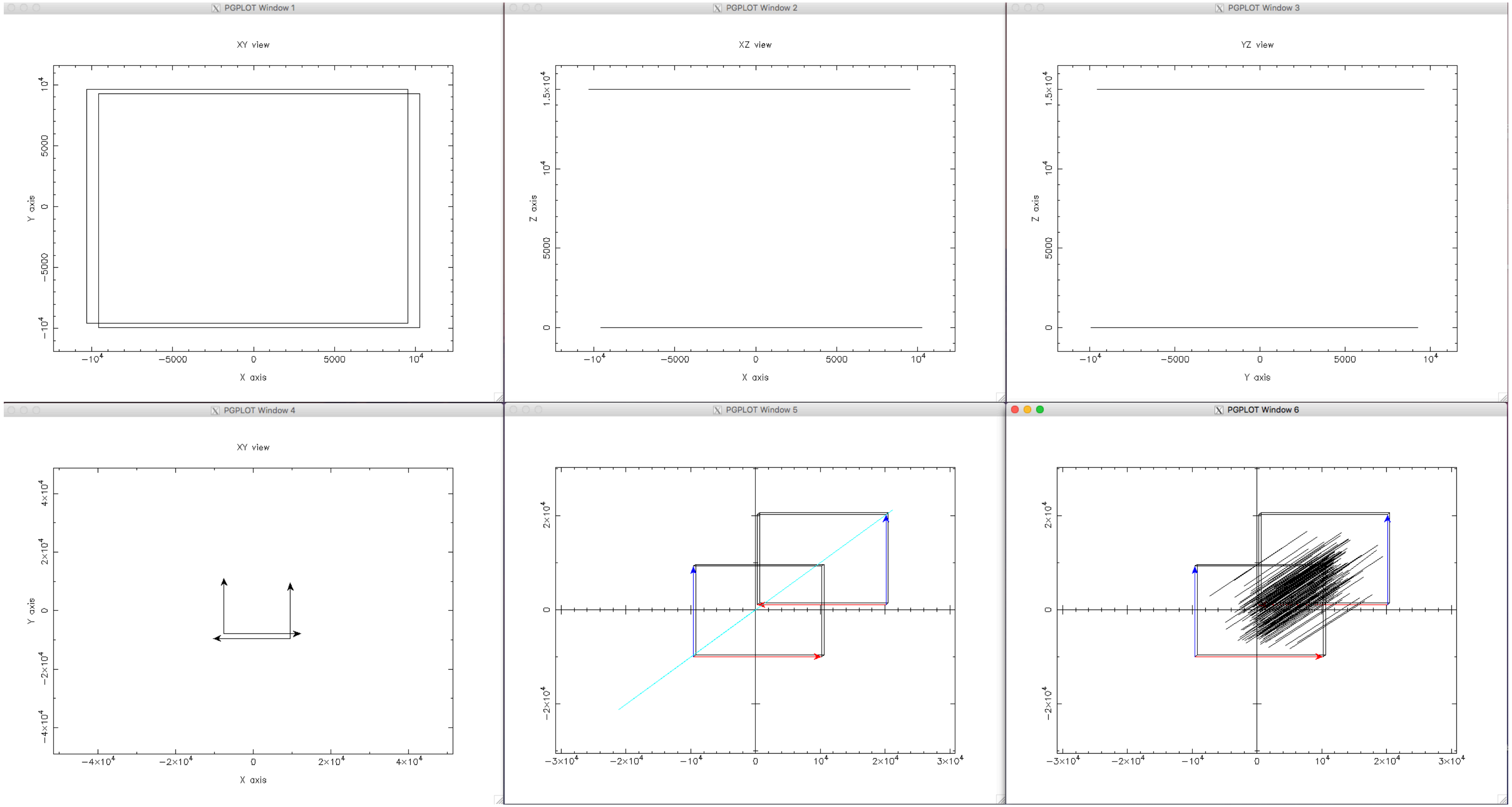

# FOOT overall detector schematic picture

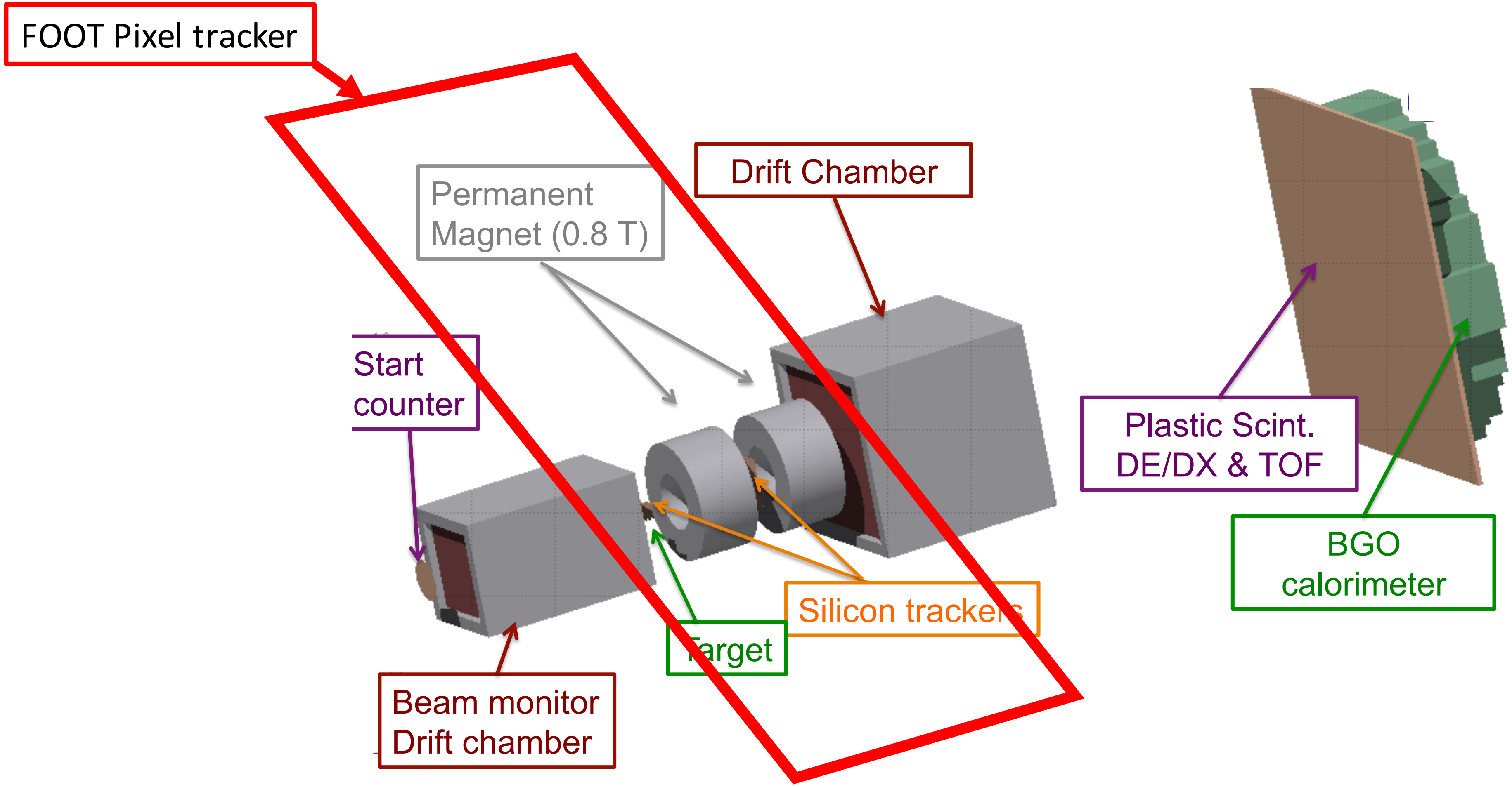

# The FIRST target and Vertex setup

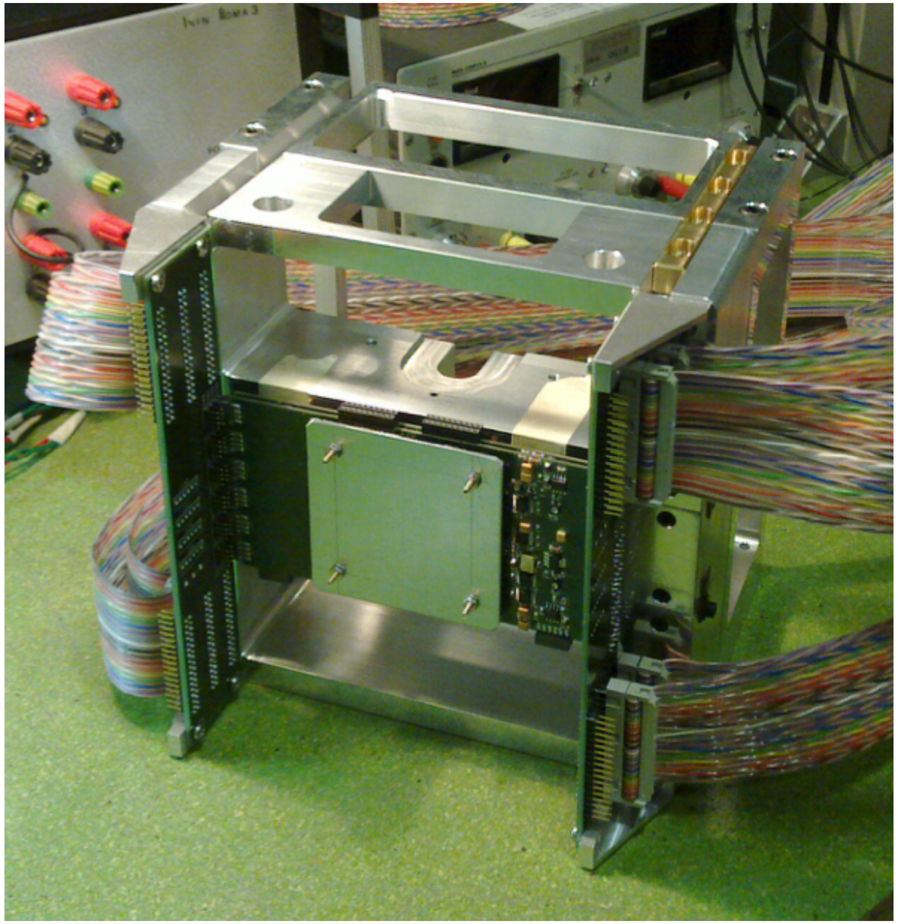

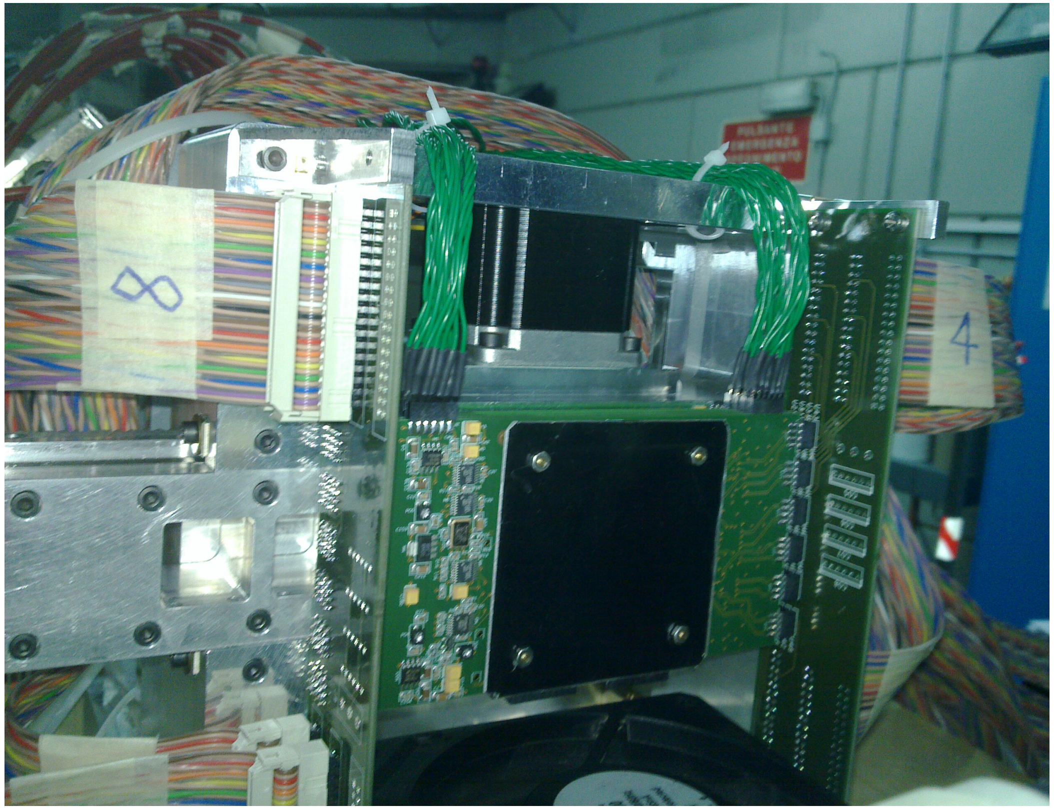

# New M28 sensor holding PCB designed for PADME/FOOT

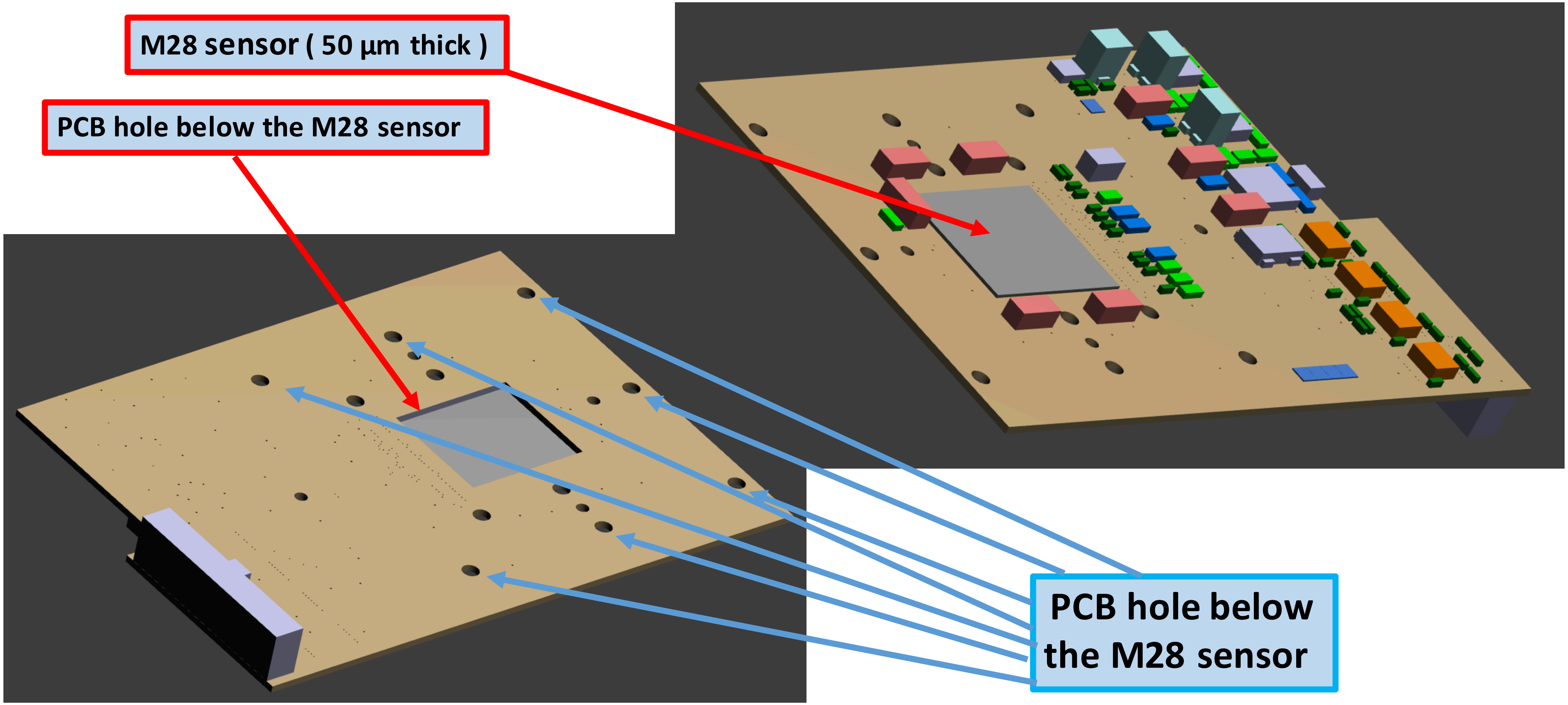

# New M28 sensor holding M28 board for PADME/FOOT

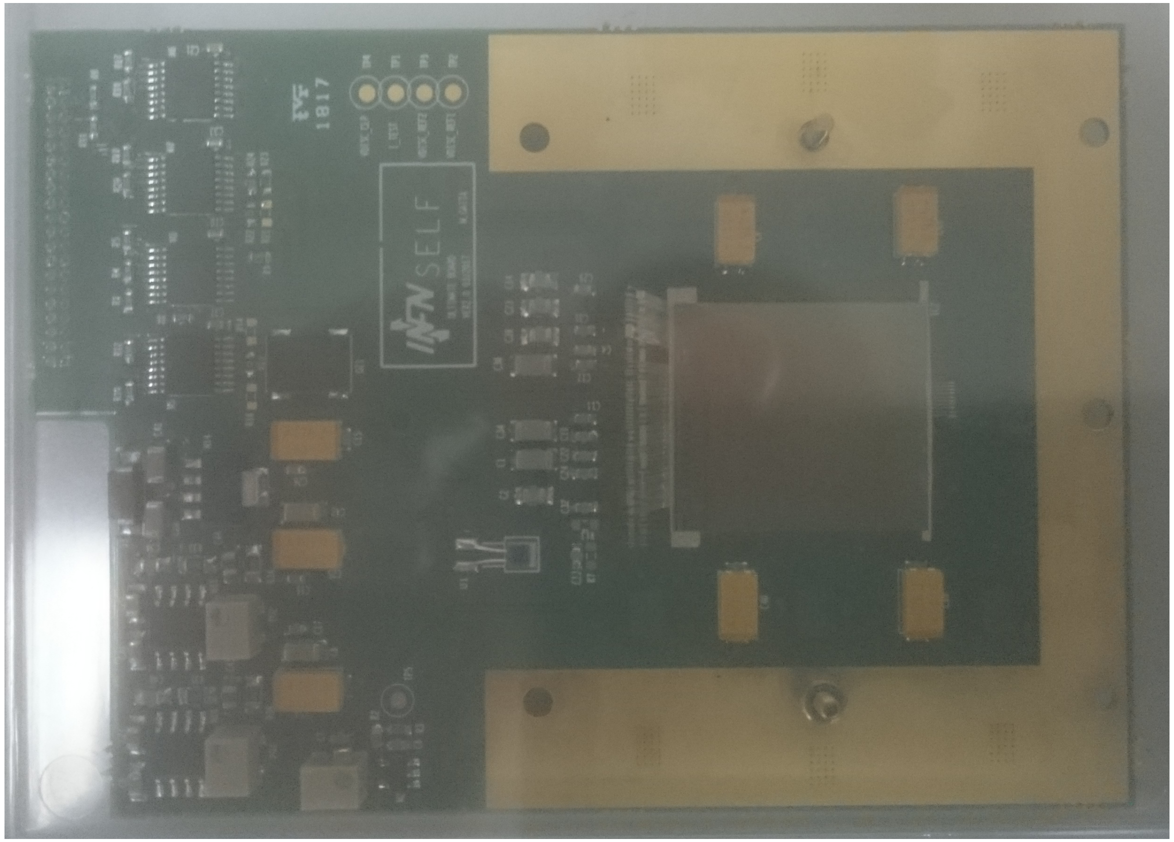

Tested in laboratory in Strasbourg mid of last june.

------

Two boards available, more in production.

------

To be tested in vacuum (for PADME) and on beam in the fall 2017.

------

**All needed functionality for FOOT already verified.**

# M28 sensor beam monitoring mechanics for PADME

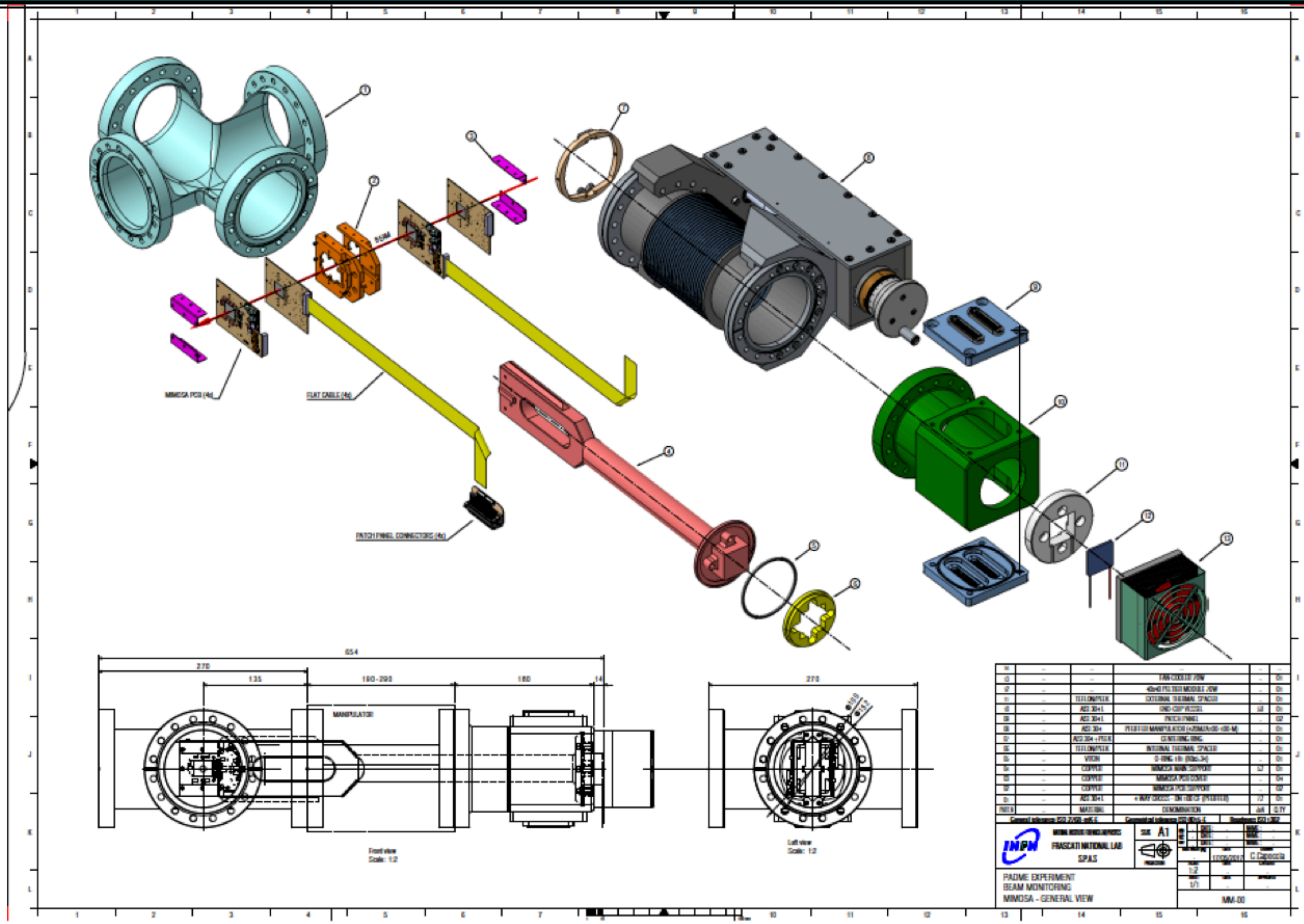

# The FOOT tracker magnetic region

INFN Istituto Nazionale di Fisica Nucleare
LABORATORI NAZIONALI DI FRASCATI
SIDS-Pubblicazioni

LNF–XX/YY(IR)
May 6, 2017

## Studio di fattibilità dei magneti in configurazione "Hallbach" dello spettrometro dell'esperimento FOOT

Claudio Sanelli[1]
[1] *INFN, Laboratori Nazionali di Frascati, I-00044 Frascati, Italy*

**Abstract**

Questa nota presenta uno studio di fattibilità per dei magneti permanenti da utilizzare nella costruzione dello spettrometro dell'esperimento FOOT. Vengono presentate simulazioni magnetiche in 2D e 3D per differenti configurazioni dei magneti permanenti in configurazione "Hallbach" facendo una valutazione comparativa delle dimensioni necessarie, in particolare per il materiale magnetico, per ottenere i valori di campo richiesti. Infine si presenta una simulazione di un sistema di due magneti così come al momento si pensa di realizzare il sistema finale dell'esperimento.

# The FOOT tracker magnetic region

**Examples of permanent magnets, Dipole and quadrupole, designed and built at LNF for DAFNE )**

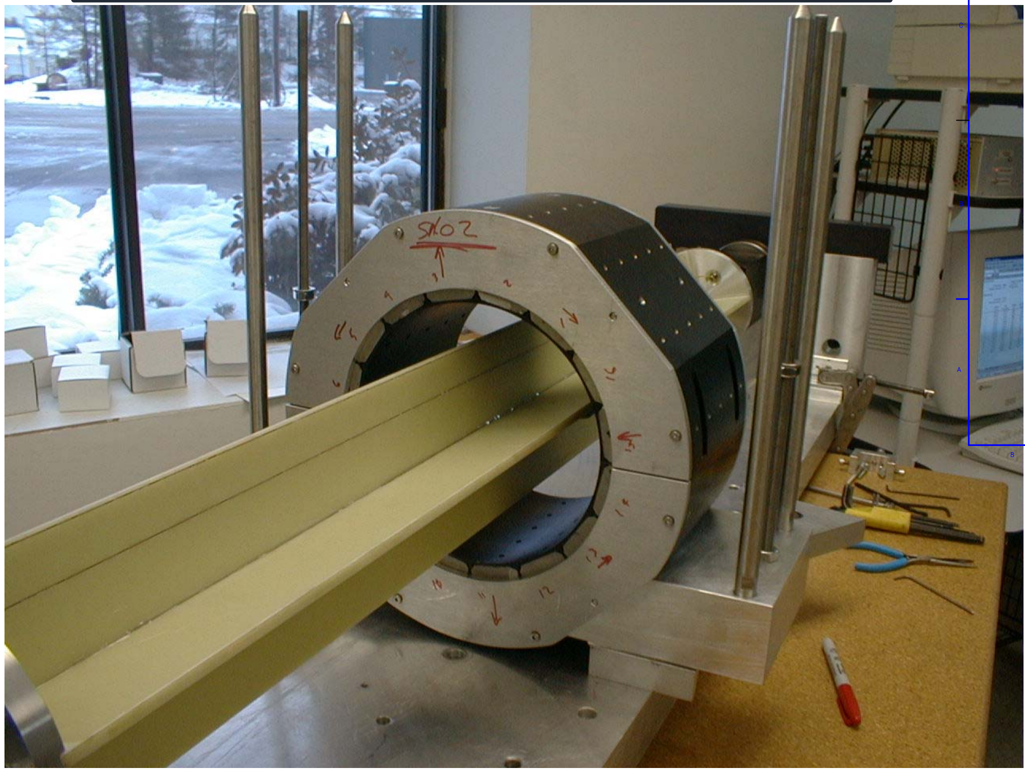

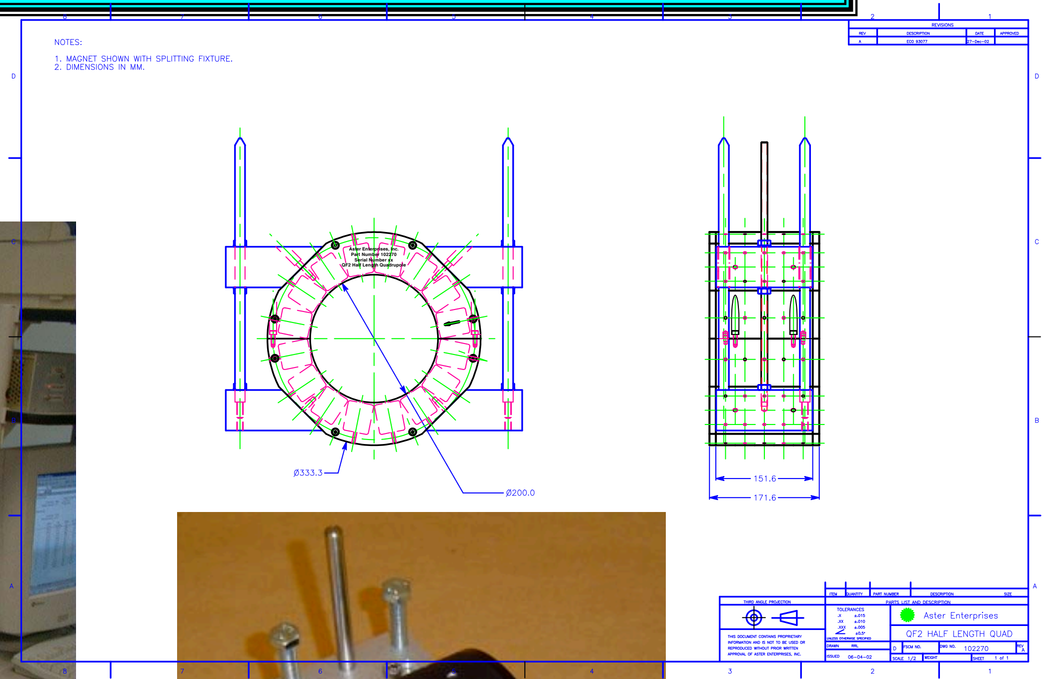


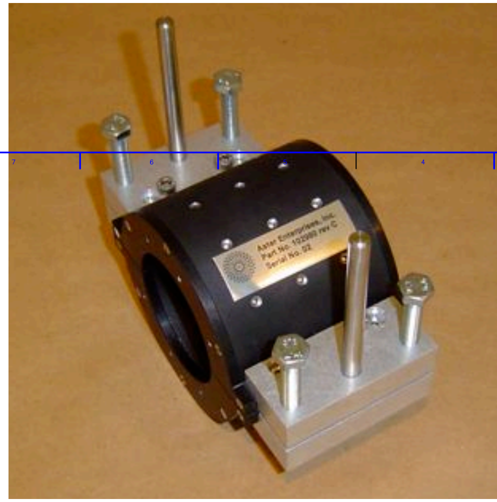

# The FOOT tracker magnetic region

Transversal dipole magnetic field in the 8 and 12 single Permanent Magnet Hallbach configurations

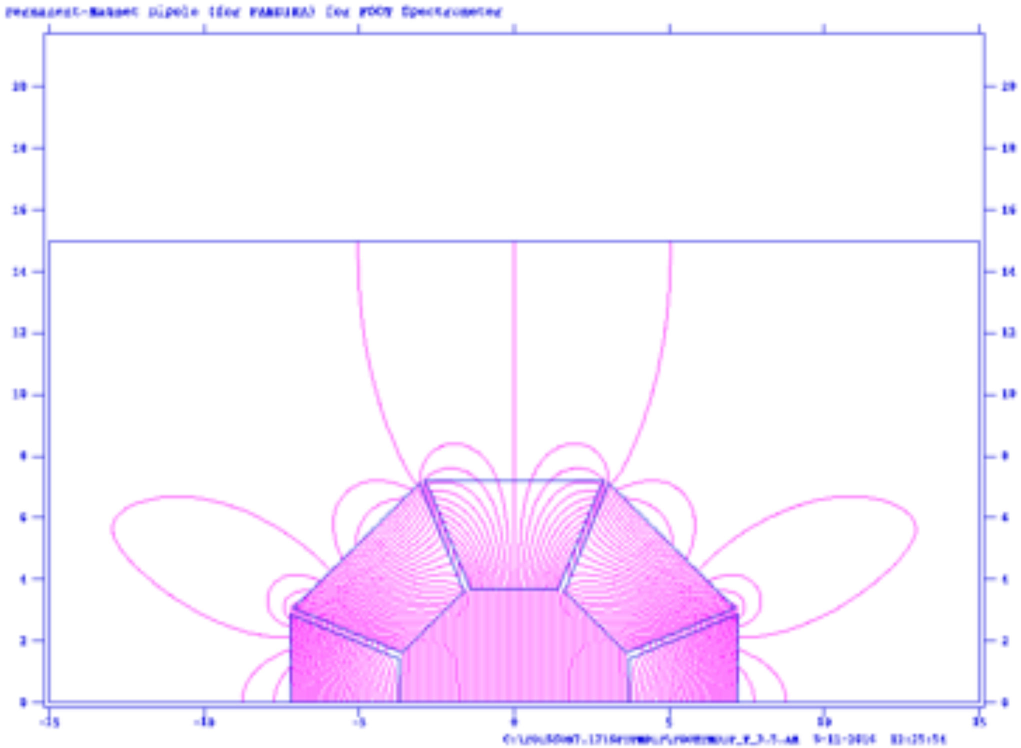

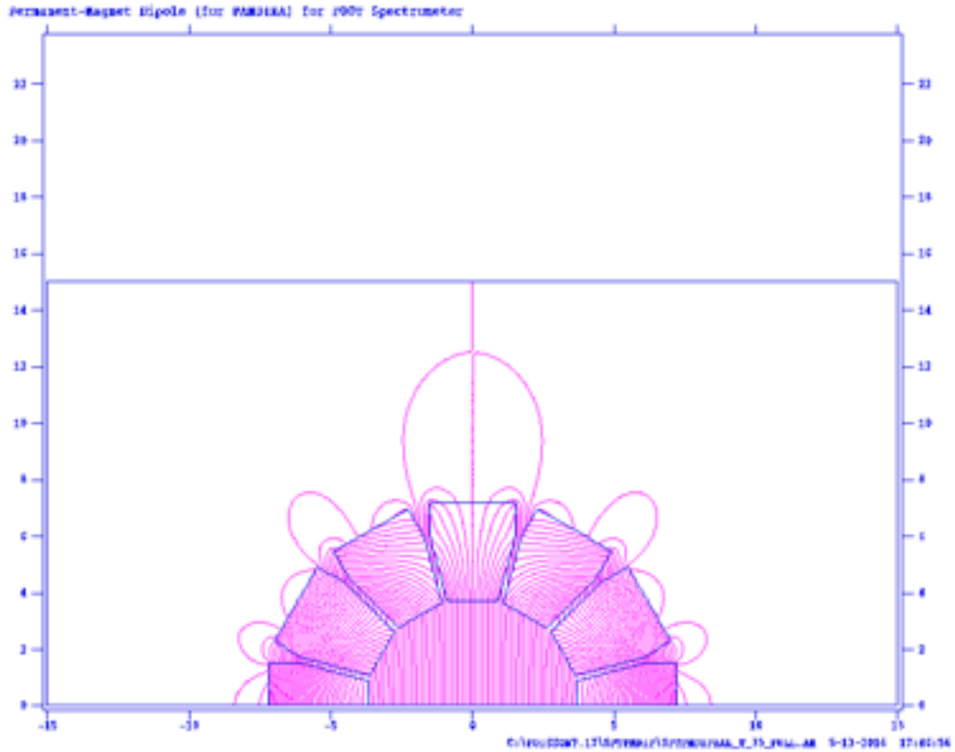

# The FOOT tracker magnetic region

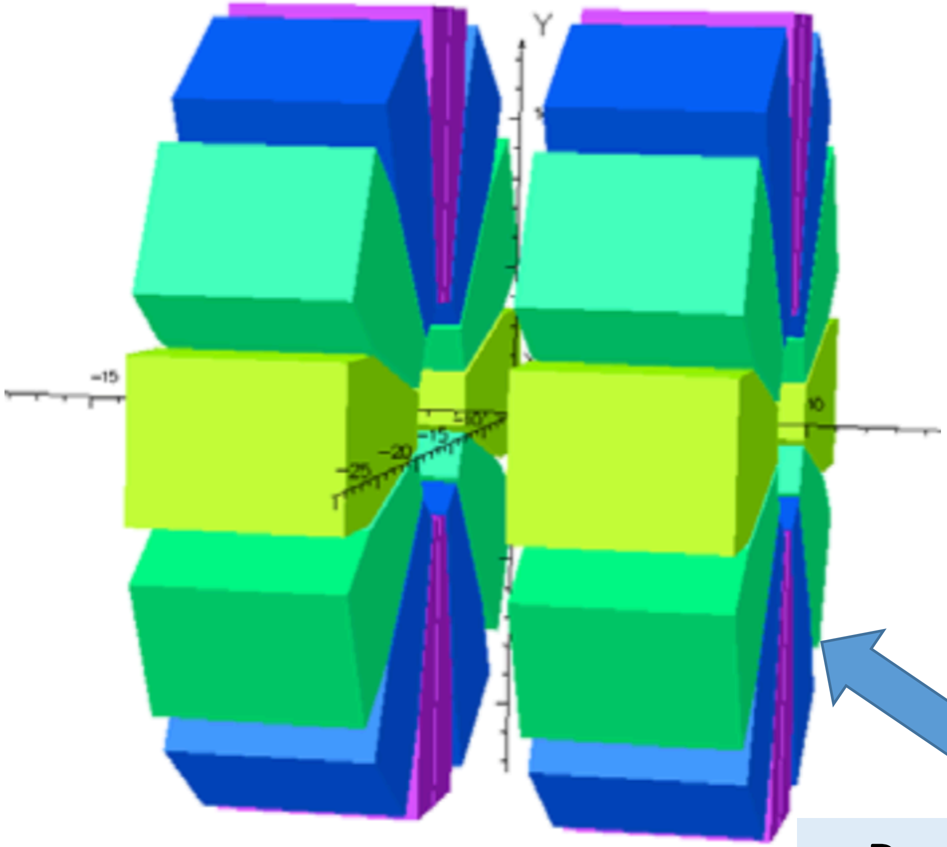

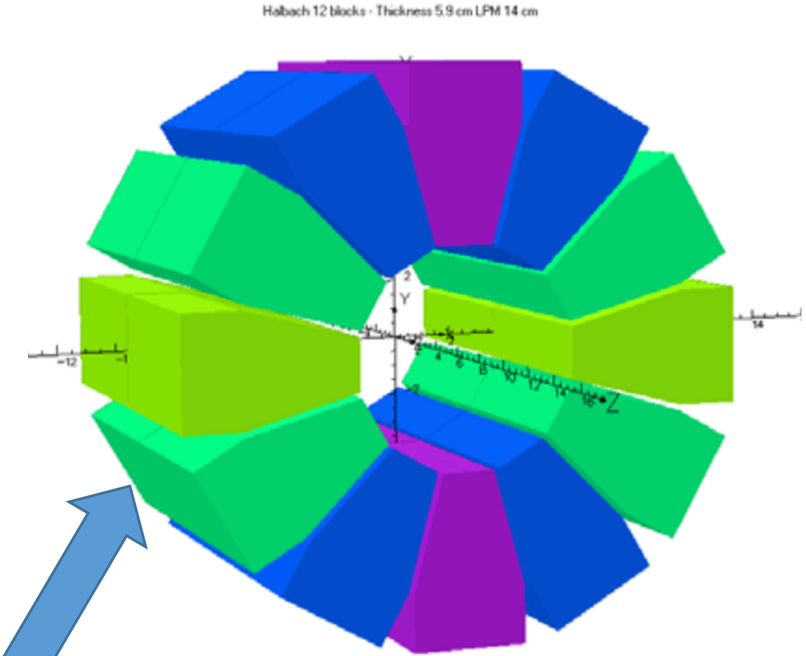


Hallbach configuration

Double magnet structure

# The FOOT tracker magnetic region

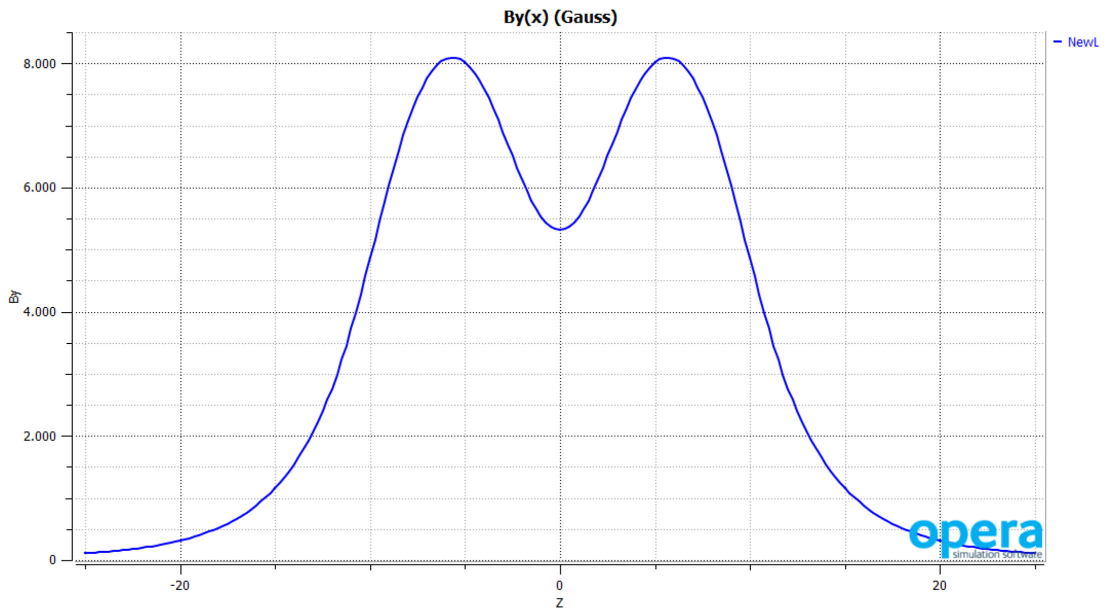


W. de Boer et al. / Nuclear Instruments and Methods in Physics Research A 487 (2002) 163–169

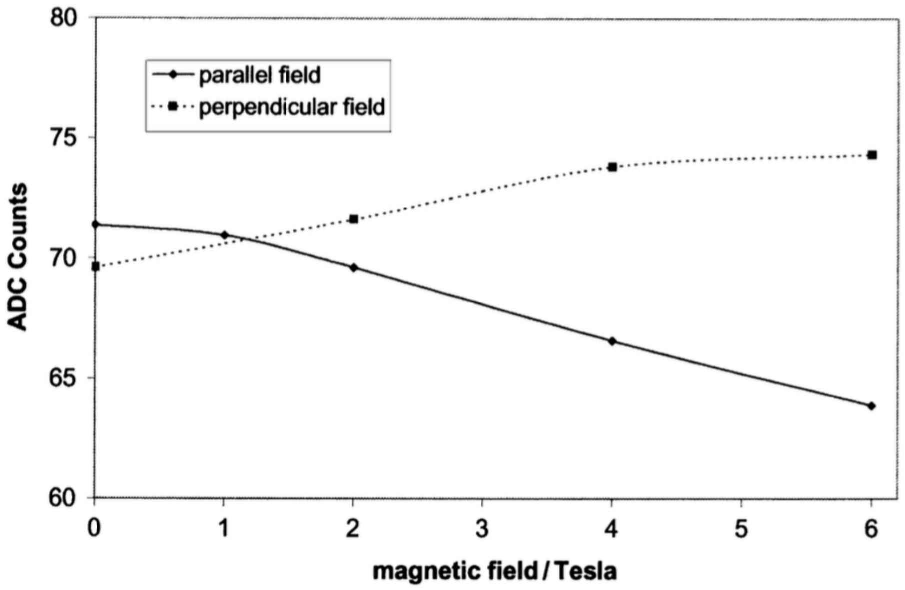


Most probable pulse height of the central pixel as function of the magnetic field parallel and perpendicular to the surface of MIMOSA.

# FOOT Inner tracker

## The basic building block idea: the PLUME module

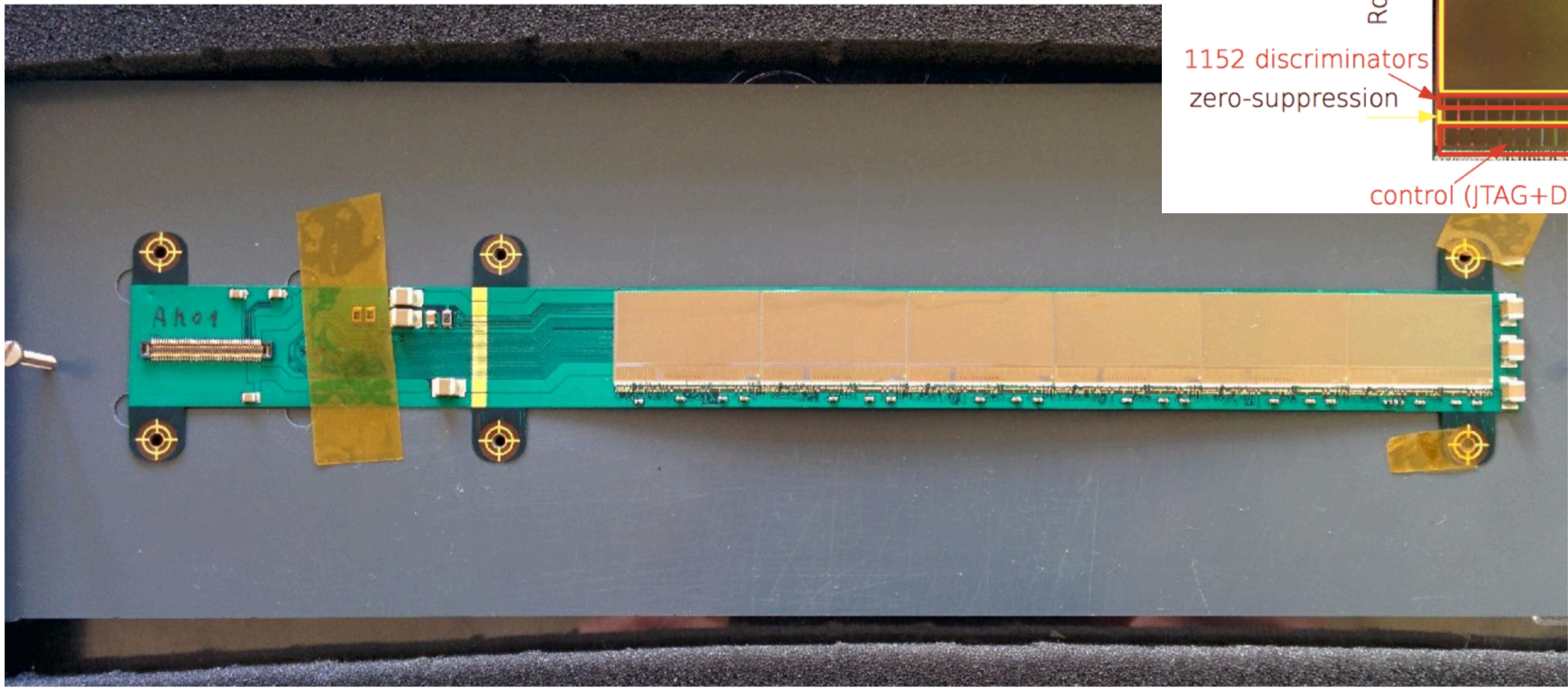


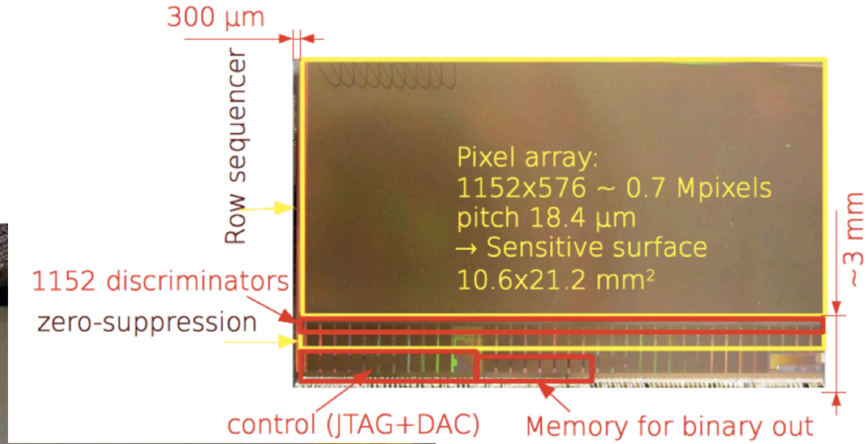

# FOOT Inner tracker

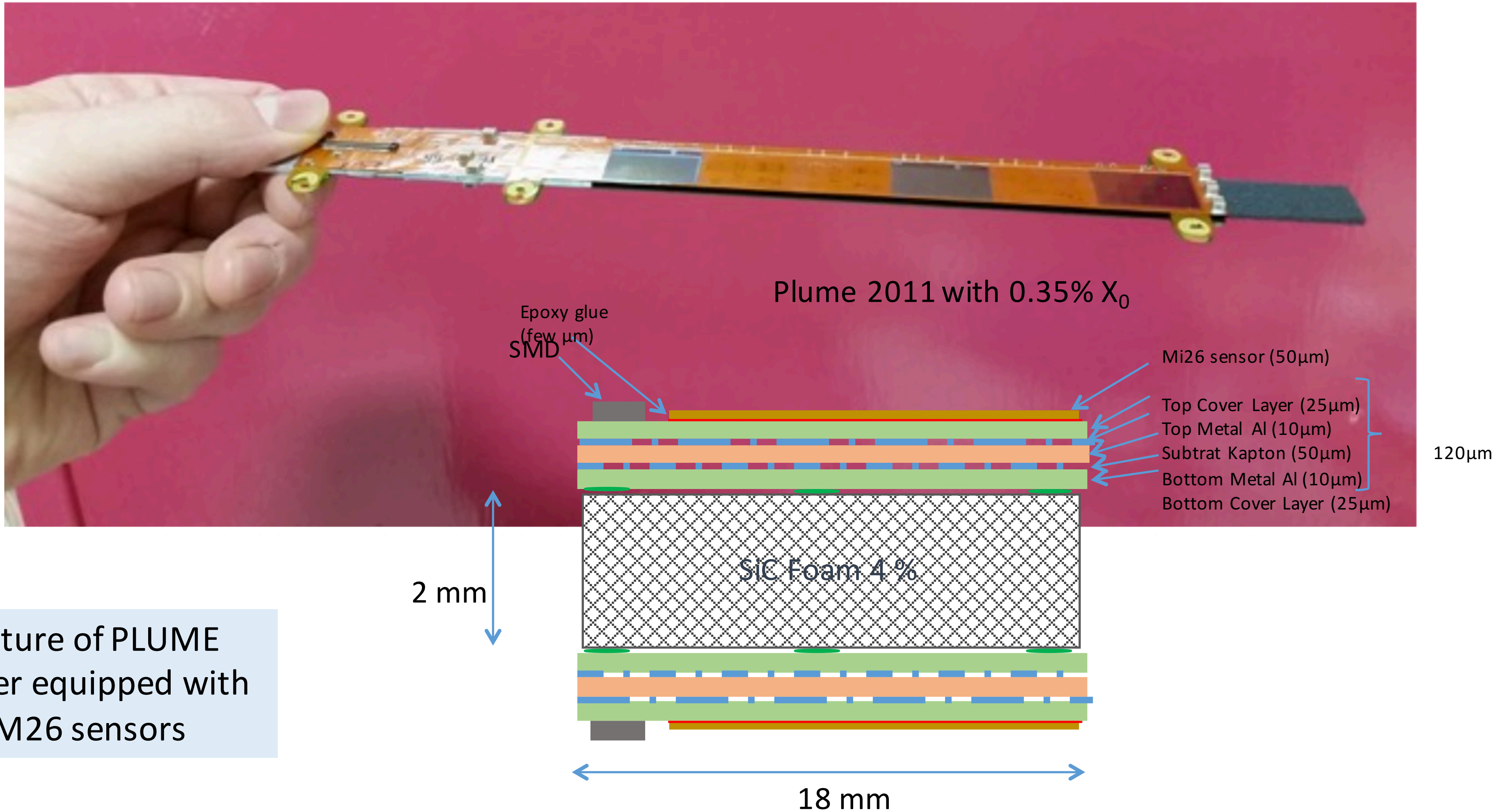


Picture of PLUME ladder equipped with M26 sensors

# FOOT Inner tracker

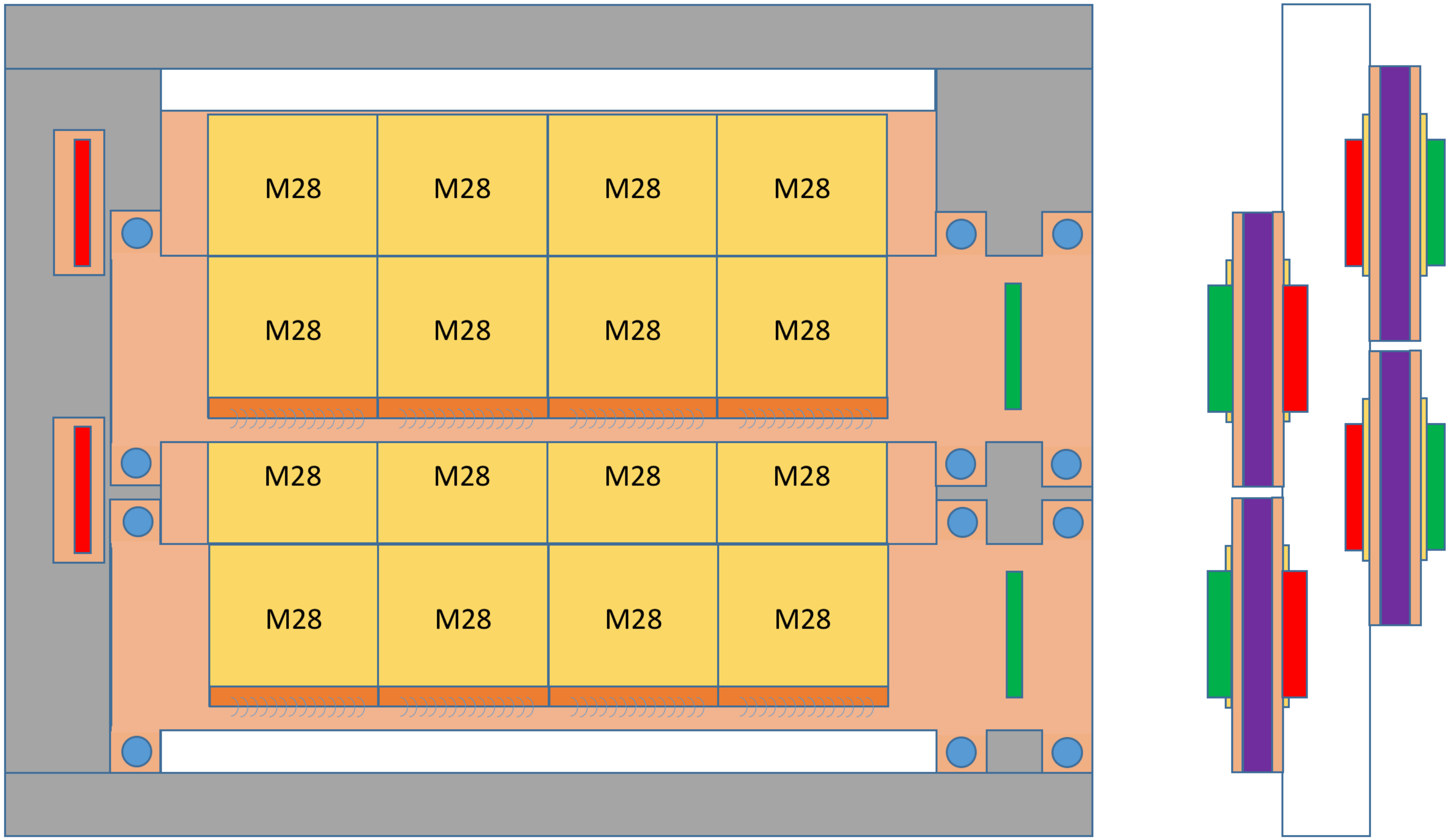

# FOOT Inner tracker DAQ


Altera Arria10 SOM board as basic building block for the Inner Tracker readout.
One board per ladder ( 8 M28s ) readout.
Needed one adapter card per board to be developed.

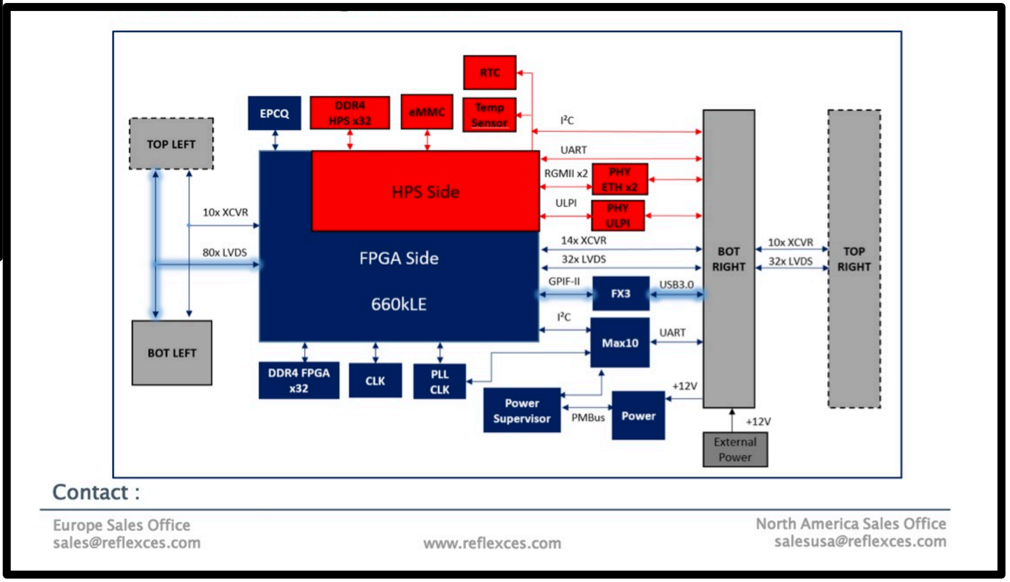

# FOOT Pixel Tracker CDR ( one )

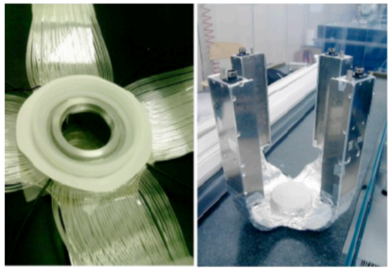

*Figure 13* – Details of the Start Counter: the thin scintillator foil and the optical bers grouped in four di erent arms.

Cortex-A9 running the data acquisition program that was connected to the outside world by a GigaBit Ethernet interface. In Fig. 17 we show the results: in the first two plots the beam profile in the two M28 sensors ( axis in $\mu$m ) and in the last one on the right the reconstructed angular divergence of the beam in mRadiants. Obtaining this result required to implement the software analysis code to do the cluster reconstruction, the alignment of the two sensor ant then the tracking to evaluate each singole track deflection angle.

### *3.2.2. Intermediate Magnetic Region*

A key ingredient element for the FOOT spectrometer is of course the magnetic system used to bend the fragments produced in the target. The main constrains driving the solution to implement are the momentum resolution at the level of few percent and the portability of the system. We'll briefly discuss both.

The momentum resolution is defined by the measurement constrains in identifying the atomic mass an number for the different fragments and the original projectile like Carbon, Oxigen and eventually Iron and by the resolution in momentum needed to reconstruct with the inverse kinematic approach the LET ( Linear Energy Transfer ) of the fragments produced by protons in the Hadrontherapy treatment. Moreover for the direct fragmentation measurements, we also plan to do, the momentum resolution is essential for the final double differential cross section precision we aim.

The portability of the system is also essential. Even though our preferred place to do the measurements is the CNAO in Pavia, we also plan other places like GSI in Darmstadt, the center of proton therapy in Trento and eventually others. Then the portability characteristic is an issue and the main element, also the Calorimeter is relevant from this point o view, is the way we implement the magnetic field forcing the choice of the permanent magnets that could allow the needed $B * L$ in a limited dimension and weight.

A preliminary feasibility study has been done to evaluate the performances we could get with this kind of solution [39]. In this study a Hallbach ( showed in Fig. 18 ) and Hallbach like configuration has been studied where the dipolar magnetic field is obtained with a cilindrical geometry

18

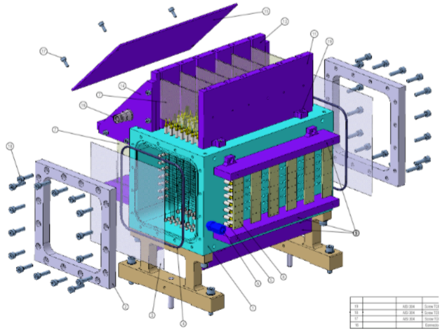

*Figure 14* – Tecnichal drawing of the BM drift chamber.

with the internal cylindrical hole is the region where the as uniform as possible constant magnetic field is obtained. The magnetic structure is composed by twelve single pieces, the material used to build them and their dimension are the main parameters that contribute to the final magnetic field obtained. For the material two options are typically available: the SmCo ( Samarium Cobalt ) and the NeFeB ( Neodymium Iron Boron ). Both the thickness of the single PM (Permanent Magnet) and the material used contribute to the field intensity produced.

Simulations, with the SmCo material, in different configurations have been done in two versions 2D and 3D. The former using the "2D Pandira" code from a general code for Permanent Magnets from the Los Alamos laboratories that provide the transversal field map for an ideal infinite length magnet, while the 3D simulations have done using the OPERA code version 16R1. Different single magnet structures have been simulated in both 2D and 3D, while a double magnet one as shown in Fig. 19 resembling the final configuration has been simulated in 3D only. The 2D simulation with a goal of 0.6 Tesla at the center of the magnet with an internal aperture of 7 cm showed possible those values with a thickness of the Permanent Magnets of 3.5 cm getting an uniformity of the magnetic field at the level of a fraction of % up to 3 cm from the central axis of the magnet. Close to the internal wall of the magnetic material the magnetic field amplitude changes ( increase or decrease depending on the configuration 8 or 12 blocks) by not more than 3.5%. Moreover the 2D simulations shows an almost linear dependence between the field amplitude at the center of the magnet versus the thickness of the magnetic material blocks that could reach 0.9 Tesla with 6.5 cm thickness.

Those numbers, as expected, changes when we move to the 3D simulation. The 3D simulation mainly produces the informations about the behaviour of the field on the axis along the magnet that for a length of the magnet similar to the internal diameter is Gaussian in shape. Like having two fringe fields joined at the center. The Maximum field at the center, with a magnet length of 9 cm and a thickness of the magnetic material of 3.5 cm like in the 2D simulation, became 0.51 Tesla. This value can be restored to 0.6 Tesla increasing the PM thickness to 4.5 cm. It can be further improved to 0.9 Tesla raising the thickness of the PM to 11 cm.

One further simulation as been done for a two magnet configuration as it will be in the final tracker. It shows, for the field along the two magnet central axis, as in Fig. 20 the sum of two

19

# FOOT Pixel Tracker CDR ( two )

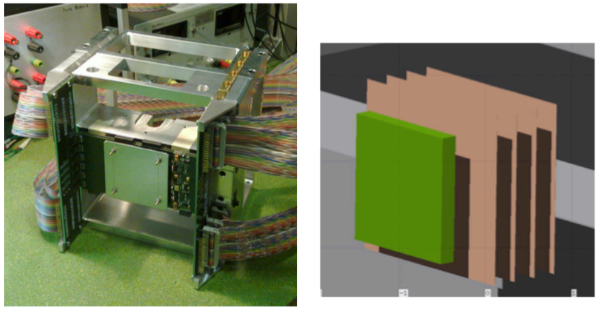

*Figure 15* – Target and vertex tracker geometrical scheme

Gaussian shaped fields indicating that the Inner Tracker, that will stand in between the two magnet, will experience a field at the level of 0.6 Tesla ( depending the distance we'll choose from the two magnets ).

All the different options simulated showed that at least in principle the level of performance we should need could be achieved at a reasonable level of weigth and dimension to cope with the need to have a portable system. Moreover we have to underline also the not trivial problems we have to face, from the point of view of the mechanical support structure, concerning the quite relevant forces that such an amount of permanent magnetic material will produce. Nonetheless to say also the impact on the precision and robustness of the mechanics needed to maintain the typical spatial resolution of pixels sensors that in our case is well below 10$\mu$m. As last remark we need also to underline the needs of a precise mapping of the field that can be done with the tools already available and used at the Frascati Laboratory.

### *3.2.3. Inner Pixel Tracker*

The FOOT Inner Tracking station foresee two planes of pixel sensors to measure both the position of the track in the plane orthogonal to the beam axis and the direction of the track itself. While the alignment of the two sensing planes can be reconstructed from the data, their distance cannot, this requires to fix them mechanically in a precise defined way using a spacer how will be explained in the construction procedure later described.

We will cover an area of about 8 cm x 8 cm in between the two permanent magnets that foresee at the moment an aperture of 5 cm and 9.2 cm in diameter respectively. Moreover, even though in this position the residual magnetic field is not negligible as shown in the plot of Fig. 20, the performances of those kind of sensors should not be affected in a relevant way as shown in reference [41]. We plan to use two planes of four times four M28 sensors, each sensor covers about 2 x 2 cm square. The use of the same technology we have in the vertex will stronghly simplify the DAQ, the procurement of the sensors, and in general will not double the need to gain the sensor specific know-how. Of course the main motivation to use the M28 sensors thinned to 50 $\mu$m is the essential advantage of minimizing the multiple scattering and nucleus refragmentation like in the Vertex. In this respect the performances will be sligthly worse because the mechanical arrangement, due to the much larger area to cover, will introduce some more material to hold the



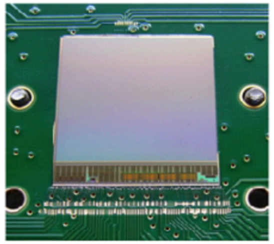

*Figure 16* – M28 pixel sensor picture

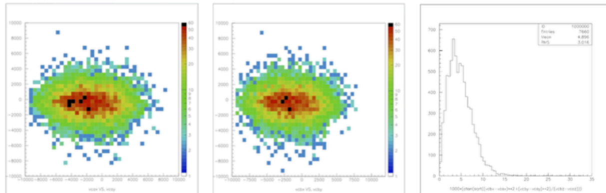

*Figure 17* – Beam profile in the two M28 sensors (left and center panel; axis in $\mu$m). Right panel: reconstructed angular divergence of the beam in mRadiants.

sensors themselves and the support to fix the distances the two planes. Moreover the material budget will also increase due to the need to cover the dead ( not sensing ) area of the sensors, expecially at the bottom where the readout logic is placed, superimposing two ladders in those areas as described later in the overall Inner Tracker geometry description.

Our proposal is to implement a structure composed by ladders similar to the ones implemented in the PLUME project [40] that can be seen in Fig. 21. In PLUME, a project started at IPHC Strasbourg in collaboration with the University of Bristol and DESY in Hamburg, a ladder is composed by two modules housing six M26 Mimosa pixel sensors each implement a double plane tracker.

While in PLUME they align 6 M26 sensors in our arrangement we will have four M28 sensors in one module. Each ladder will see two modules face to face, and four ladders will be placed on a metallic frame to hold the entire tracker as in the arrangement depicted in Fig. 22 where we can see a principle scheme about the way we propose to implement the Pixels Inner Tracker. We have four ladders: two placed on the front side of the metallic support frame ( gray color in the scheme ) and two on the opposite side.

# FOOT Pixel Tracker CDR ( three )

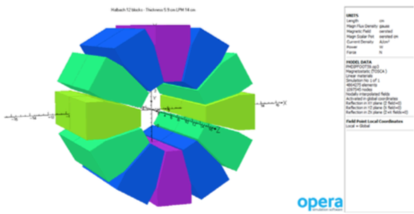

*Figure 18* – Typical Hallbach configuration with 12 single magnetic material pieces

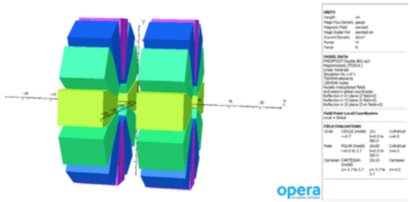

*Figure 19* – Double magnet picture

A single module is based on a FPC ( Flexible Printed Cable ) made in Kapton having two or three conductive planes with an overall thickness of the order of 100 $\mu$m, then the four sensors will be glued on it and then bonded. The distance from two consecutive sensors in the module can be limited to about 30 $\mu$m, as has been achieved in the PLUME project, to minimize the horizontal dead area. The top side of the sensor will be aligned with the border of the FPC while on the bottom one the FPC will stand few millimeters longer than the sensor to allow enough room for the bonding pads. The Kapton cable will have one or two SMD low insertion force connectors to manage the power supply, control and data signals from and to the sensors. The use of one or two connector will be decided following the constrains for the final design, placing them eventually one on each end of the FPC ( solution not shown in the picture ). This has not been done in the PLUME project due to the specific requirements due to the application of monitoring the beam background for the Belle II experiment.

At the end of the sensors row the support Kapton cable will last longer than the sensors. Those two "tails" on one side, the left one in the Fig. 22 will have two "ears" to fix the ladder to the metallic support structure, on the right side the tail is longer with four "ears" again to hold the system and to accomodate the connector/connectors for the sensors control. A spacer 2 mm thick made of a special SiC foam with very low density, in reference [42] can be found the characteristics of the foam used in the PLUME project, will be used as spacer to define the distance of the two planes. On this spacer two modules, oriented with the sensors on the external sides, will be glued. The dead area due to the readout electronic region at the bottom of the sensors will superimpose, while horizontally the sensor will be shifted by few hundreds of $\mu$m to avoid the superimposition

22

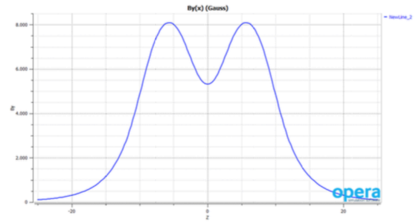

*Figure 20* – Longitudinal magnetic field amplitude ( Gauss ) along the axis of the two magnets system

*Figure 21* – Picture of a PLUME ladder

of the dead area from one sensor and the following. This assembly procedure will require to design and realize a specific mechanical jig and specific know how that we have already identified in an external company with years of experience in this kind of activities [43].

On the rigth side of picture in Fig. 22 we see how the four modules are located in the global structure. Each module has two connectors, in red and green color, respectively on the front and back side of the ladder. One for module.

The ladders in the front side of the frame are fixed with the end side housing the connector on the rigth hand side of the structure, while the other two on the back of the frame in the opposite orientation. In this condition we'll need to reach the back side connector (red color) of the ladders placed on the side of the FPC touching the mechanical support structure through four buttonholes in the structure itself. This is shown in the left side of the left figure while the other two on the back side on the two ladder placed in the front side of the mechanical structure are not visible because behind the FPC and connector shown on the right side of the left figure. The two buttonholes in the left side can be identified by the two red rectangles representing the connectors above the orange colored layer representing the FPC surrounded by grey area showing the mechanical support.

### *3.3. Downstream Tracking: the Drift Chamber*

Tracking of fragments downstream the magnetic volumes is essential for the measurement of momentum and is also fundamental to match the reconstructed tracks with the hits in the TOF scintillator and the calorimeter. The choice of a gas detector is considered ideal in order to provide a sufficient spatial resolution and, at the same time, to minimize the amount of material, thus reducing both the impact of multiple scattering and also secondary fragmentation effects in the detector itself.

As a baseline option we can consider the same structure of the Beam Monitor chamber described in section 3.1, *i.e.* consecutive X-Y planes with staggered rectangular cells of size $1.6{\times}1.0$ cm$^2$, but with the difference of having a wider sensitive area, in order to cover the angular acceptance

23

# FOOT Pixel Tracker CDR ( four )

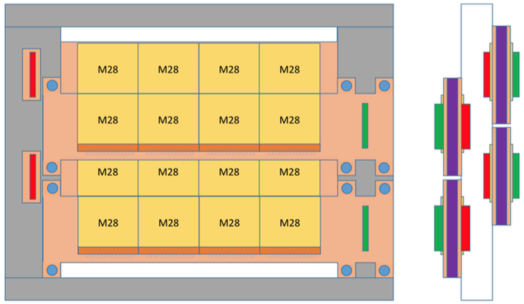


*Figure 22* – Inner tracker principle scheme

defined by the aperture of the magnetic system. The effective size of the chamber area is therefore dependent on the longitudinal positioning. The chamber has to be positioned at least about 10 cm downstream the second magnet, in order to avoid possible operation problems deriving from the fringe magnetic field. For this kind of positioning, we are considering at present a structure again with 6+6 X-Y layers, but having 8 cells per layer instead of 3 as for the Beam Monitor. The first sensitive layer is at a distance of 35 cm from the target. The entrance window is $20\times20$ cm$^2$ wide. The length of the wires is 20 cm. Fig. 23 shows a sketch taken from the simulation setup.

In this configuration the Drift Chamber has a total of 96 wires, corresponding to an equal number of readout channels, and 760 field wires (8 per cell). This design allows us to consider conservatively a space resolution of about 150 $\mu$m for a single track in a cell, according to the performance obtained in the FIRST experiment [34, 35].

With respect to the case of the Beam Monitor, it is of fundamental importance to optimize the readout of the Drift Chamber in order to have an efficient multi-track operation capability, since we expect interesting events to have multiple tracks in the tracking system. The angular separation of tracks allows to have a significant probability to efficiently identify the different particles. However in a fraction of cases there will more than one track in the same drift cell. We therefore need a multi-hit readout and different solutions are at present under study. This is a non trivial aspect for different reasons, one of the most relevant being the large expected difference of pulse amplitudes due to the different fragment charge. Multi-hit capability also depends on the time separation of pulses on the same wire, originating by simultaneous tracks in the same cell, and corresponding to different drift times. For this reason an efficient operation with the slowest possible drift velocity has to be looked for. To this purpose a careful optimization of gas mixture is under consideration. A further optimization towards a more efficient multi-track capability can be given by increasing the redundancy of space point information per layer. For instance, instead of a simple two projection X-Y orthogonal wire structure, a setup having three sets of wires at three different angles will also be studied [44]. Of course, the number of total layers can be maintained, so to keep the same number of readout channels.

24

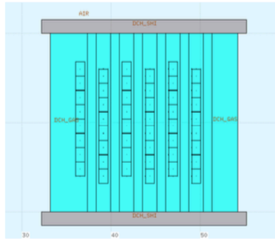

*Figure 23* – Enlarged view of the sketch of the drift chamber as taken from the simulation setup

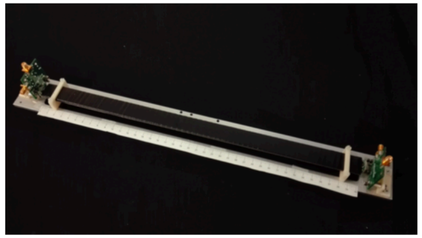

*Figure 24* – Picture of the dE/dx detector prototype.

The choice of gas mixture has also some relevance as far as multiple scattering is considered. For this reason a He-based mixture can be a possibility [45, 46]. However the study of the global track reconstruction performances (as reported in sec.7.2) already includes the impact of multiple scattering.

Simulation studies have been performed to evaluate the probability of secondary fragmentation in the chamber volume. Leaving aside the tracks that imping on the external mechanical structure of the chamber (which in any case has to be designed as lightest as possible), charged fragments may interact in the entrance or exit windows (basically Al-mylar), in the gas and against the wires. As a result we have obtained that the fraction of events where such scatterings can occur is below 0.5%. Instead, unwanted fragmentation of the external structure might exceed 1-2%. The impact of this phenomenology in the reconstruction performances has to be carefully evaluated.

*3.4. $\Delta E$ and TOF Detector*

*3.4.1. Structure of the detector*

The dE/dx detector prototype we are currently testing is composed by two layers of plastic scintillator bar coupled at both ends to silicon photomultipliers (SiPM) via optical glue (Saint-Gobain, BC-630). A picture of a single bar is shown in Fig. 24. The two layers are arranged orthogonally to identify the two-dimensional interaction position of the particle in the detector.

25

# FOOT LNF 2018 financial request

**Schema temporale attività nel triennio 2018-2020**

( I-S = Primo semestre , II-S = Secondo semestre )

| | |
|---|---|
| Gara magneti tracciatore | I-S 2018 |
| Costruzione magneti tracciatore | II-S 2018 |
| Costruzione Vertice | I-S 2018 |
| Test su fascio Vertice (BTF, LNS) | II-S 2018 |
| Acquisto secondo wafer M28 | I-S 2018 |
| Disegno e realizzazione prototipi dei moduli/ladders Inner Tracker | I-S 2018 |
| Disegno e realizzazione scheda interfaccia FPC-SOM (Inner Tracker) | I-S 2018 |
| Disegno/realizzazione frame meccanico Inner Tracker | I-S 2018 |
| Disegno meccanica supporto tracciatore | II-S 2018 |
| Test su fascio ladder Inner Tracker (BTF,LNS) | I-S 2019 |
| Costruzione ladders finali Inner Tracker | II-S 2018, I-S 2019 |
| Realizzazione meccanica supporto tracciatore | I-S 2019 |
| Mappa campo magneti tracciatore | I-S 2019 |
| Assemblaggio meccanico tracciatore | II-S 2019 |
| Prima presa dati con tracciatore al GSI | II-S 2019, I-S 2020 |

# FOOT LNF

# 2018 financial request

**ISTITUTO NAZIONALE DI FISICA NUCLEARE**
Preventivo per l'anno 2018

| Struttura |
|---|
| Lab. Naz. di Frascati |

| CODICE | SIGLA | COMMISSIONE |
|---|---|---|
| | FOOT | CSN III |
| Resp. Loc.: Eleuterio Spiriti | | |

## PREVENTIVO LOCALE DI SPESA (In K€)

**L'inserimento delle richieste è a carico dei responsabili locali delle CSN1,2,3,5 P.S. e C.C.R.**

**Per la CSN4, l'inserimento è a carico dei responsabili NAZIONALI e/o dei coordinatori.**
**L'accesso ai responsabili locali di CSN4 è garantito in SOLA LETTURA**

| Capitolo | *Descrizione* | Parziali | | Totale | |
|---|---|---|---|---|---|
| | | Richiesta | SJ | Richieste | SJ |
| MISSIONI | 1. Test beam LNS ( 2 persone per 1 settimana ) | 2.00 | | | |
| | 2. Viaggi a Strasburgo | 2.00 | | | |
| | 3. Viaggio presso ditta magneti | 1.00 | | | |
| | 4. Due riunioni di collaborazione (2 persone x 3 giorni a riunione) | 2.00 | | | |
| | 5. Viaggi presso altre sedi dell'esperimento | 1.00 | | 8.00 | 0.00 |
| MISSIONI | | | | | |
| CONSUMO | 1. Prototipo FPC Kapton Inner Tracker FOOT ( attrezzatura + realizzazione). Stima da quotazione ARTEL Srl. | 1.00 | | | |
| | 2. Prototipo FPC Kapton Inner Tracker FOOT ( 2 esemplari, attrezzatura + montaggio). Stima da quotazione ARTEL Srl. | 1.00 | | | |
| | 3. Incollaggio e bonding M28 per prototipo Inner Tracker (costi non ricorrenti). Stima da quotazione G&A Engineering. | 4.00 | | | |
| | 4. Incollaggio e bonding M28 per prototipo Inner Tracker (costi ricorrenti). Stima da quotazione G&A Engineering. | 2.50 | | | |
| | 5. SiC foam per costruzione Ladders Inner Tracker (www.ERGaerospace.com/SiC-properties.htm). Stima dei costi dal gruppo di Strasburgo. | 2.00 | | | |
| | 6. Scheda interfaccia FPC-SoM (prototipo PCB, attrezzatura + PCB). Stima da SEA LNF (Servizio Elettronica ed Automazione LNF). | 2.00 | | | |
| | 7. Scheda interfaccia FPC-SoM (montaggio prototipo, attrezzatura+montaggio). Stima da SEA LNF (Servizio Elettronica ed Automazione LNF). | 2.00 | | | |
| | 8. Costruzione frame meccanico Inner Tracker | 2.00 | | 16.50 | 0.00 |
| CONSUMO | | | | | |
| ALTRI_CONS | | | | | |
| TRASPORTI | 1. Trasporti a LNS per test beam | 1.00 | | 1.00 | 0.00 |
| TRASPORTI | | | | | |
| PUBBLICAZIONI | | | | | |
| MANUTENZIONE | | | | | |
| INVENTARIO | 1. http://www.mouser.it/ProductDetail/ReFLEX-CES/RXCA10S066PF34-IDK0SA/?qs=VWNNG7jHlrJAgnf6H0LL3w== | 3.00 | | 3.00 | 0.00 |
| INVENTARIO | | | | | |
| APPARATI | 1. Magnete 1 (tra vertice e inner trarre). Stima da quotazione budgetaria: Electron energy corporation (www.electronenergy.com) | 40.00 | | | |
| | 2. Magnete 2 (tra vertice e Inner Tracker). Stima da quotazione budgetaria: Electron energy corporation (www.electronenergy.com) | 50.00 | | | |
| | 3. Acquisto secondo wafer sensori M28 ( da Strasburgo ). Stessi costi acquisto primo wafer nel 2017 | 25.00 | | | |
| | 4. Produzione PCB per Vertice FOOT ( attrezzatura + realizzazione). Stima da quotazione ARTEL Srl. | 1.00 | | | |
| | 5. Montaggio PCB per Vertice FOOT ( 5 esemplari, attrezzatura + montaggio). Stima da quotazione ARTEL Srl. | 1.50 | | | |
| | 6. Incollaggio e bonding M28 per Vertice (costi non ricorrenti). Stima da quotazione G&A Engineering. | 4.00 | | | |
| | 7. Incollaggio e bonding M28 per Vertice (costi ricorrenti). Stima da quotazione G&A Engineering. | 1.50 | | | |
| | 8. Realizzazione FPC Kapton Inner Tracker FOOT ( attrezzatura + realizzazione). Stima da quotazione ARTEL Srl. | 1.00 | | | |
| | 9. Realizzazione FPC Kapton Inner Tracker FOOT ( 5 esemplari, attrezzatura + montaggio). Stima da quotazione ARTEL Srl. | 1.00 | | | |
| | 10. Incollaggio e bonding M28 per prototipo Inner Tracker (costi non ricorrenti). Stima da quotazione G&A Engineering. | 4.00 | | | |
| | 11. Incollaggio e bonding M28 per prototipo Inner Tracker (costi ricorrenti). Stima da quotazione G&A Engineering. | 10.00 | | | |
| | 12. Scheda interfaccia FPC-SoM (PCB, attrezzatura + PCB). Stima da SEA LNF (Servizio Elettronica ed Automazione LNF). | 2.00 | | | |
| | 13. Scheda interfaccia FPC-SoM (montaggio, attrezzatura+montaggio). Stima da SEA LNF (Servizio Elettronica ed Automazione LNF). | 2.00 | | | |
| | 14. 5 schede SOM con FPGA Arria10 Altera con costi e caratteristiche da: http://eu.mouser.com/ProductDetail/ReFLEX-CES/RXCA10S066PF34-SOM00T/?qs=%2fha2pyFaduiipVquB0Q9dE1nJypRzVABapOM8AL4dF9aYunLQbRN2YxnBwNzYg%252bx | 10.50 | | 153.50 | 0.00 |
| APPARATI | | | | | |
| LICENZE-SW | | | | | |
| SPSERVIZI | | | | | |

Mod. EC/EN 2 (a cura del responsabile locale)

# Conclusions

## A lot of work in front of us!

### 2017 main activities

- Test of the new M28 sensor board ( test @ BTF and, if possible @ LNS )
- Improvement of the new SoC DAQ ( in vacuum for PADME )
- Study of a possible mechanical solution of the Inner Tracker
- Tentative design of the new kapton FPC ( Flexible Printed Cable ) for the FOOR version of the PLUME ladder
- Interaction with G&A Engineering for a preliminary cost estimation

### 2018 main activities

- Assembly of the new M28 ladder prototype
- Definition and building of the new DAQ for the Inner Tracker
- Study of the solution of the entire Tracker mechanics
- Bid for the two magnets and mapping
- Building of the final Inner Tracker
- Test of the different components